GEOLOGIJA *62/2*, 153–173, Ljubljana 2019
© Author(s) 2019. CC Atribution 4.0 License

https://doi.org/10.5474/geologija.2019.007

Triassic deep-water sedimentation in the Bled Basin, eastern Julian Alps, Slovenia

Triasna globljevodna sedimentacija v Blejskem bazenu, vzhodne Julijske Alpe, Slovenija

Luka GALE[1,2], Tea KOLAR-JURKOVŠEK[2], Barbara KARNIČNIK[3], Bogomir CELARC[2], Špela GORIČAN[4] & Boštjan ROŽIČ[1]

[1]Univerza v Ljubljani, Naravoslovnotehniška fakulteta, Oddelek za geologijo, Aškerčeva 12, SI-1000 Ljubljana, Slovenia; e-mail: luka.gale@geo-zs.si
[2]Geološki zavod Slovenije, Dimičeva ulica 14, SI-1000 Ljubljana, Slovenia
[3]Škalska cesta 9, 3320 Velenje, Slovenija
[4]ZRC SAZU, Paleontološki inštitut Ivana Rakovca, Novi trg 2, SI-1000 Ljubljana, Slovenia

Prejeto / Received 3. 10. 2019; Sprejeto / Accepted 7. 11. 2019; Objavljeno na spletu / Published online 24. 12. 2019

Key words: Upper Triassic, Southern Alps, paleogeography, conodonts, radiolarians
Ključne besede: zgornji trias, Južne Alpe, paleogeografija, konodonti, radiolariji

Abstract

The Bled Basin was a Middle Triassic–Early Cretaceous basin whose remnants are preserved in the eastern Southern Alps in western Slovenia. The early evolution of the basin is recorded in the Upper Ladinian to Lower Jurassic Zatrnik cherty limestone formation, which in the Pokljuka Nappe overlies Middle Triassic volcanics, volcaniclastics and hemipelagic limestones. The Zatrnik Limestone is poorly documented and biostratigraphically not well constrained. The base of the Zatrnik Limestone was logged in four sections in the eastern part of the Pokljuka plateau. An Upper Ladinian *Muelleritortis cochleata* Radiolarian Zone was recognised in the lowermost part, whereas conodont data indicate Julian to latest Tuvalian/early Norian age for the rest of the logged sections. Microfacies analysis indicates hemipelagic deposition on a basin plain and/or distal slope, which is often interrupted by distal calciturbidites.

Izvleček

Blejski bazen je bil srednjetriasni do zgodnjekredni globljemorski sedimentacijski prostor, katerega ostanki so ohranjeni v Pokljuškem pokrovu vzhodnih Južnih Alp v zahodni Sloveniji. Zgodnji razvoj bazena je zabeležen v srednjetriasnih vulkanitih, vulkanoklastitih in hemipelagičnih apnencih, ki jim sledi zgornjeladinijska do spodnjejurska formacija Zatrniškega apnenca z roženci. Zatrniški apnenec je sedimentološko in biostratigrafsko razmeroma slabo raziskan. V članku so predstavljeni štirje profili Zatrniškega apnenca z vzhodnega dela Pokljuke, ki zajemajo spodnji del formacije. V najnižjem delu formacije je bila določena zgornjeladinijska radiolarijska cona *Muelleritortis cochleata*, višji deli profilov pa vsebujejo julske, tuvalske in/ali spodnjenorijske konodontne združbe. Mikrofaciesi kažejo na hemipelagično in turbiditno sedimentacijo na bazenski ravnici in/ali na distalnem delu pobočja.

Introduction

Stratigraphically continuous successions of Upper Triassic hemipelagic, pelagic and gravity-flow deposits up to several hundred meters thick preserved in north-western Slovenia testify to the existence of at least three long-lived Mesozoic marine basins located near the western margin of the Neotethys Ocean. Continuous successions of Ladinian to Upper Cretaceous deeper-marine strata are mostly located in the Tolmin Nappe of the eastern Southern Alps (Buser, 1987). This basin is usually referred to as the Slovenian Basin s. str. (Cousin, 1970, 1973; Buser, 1989, 1996) or the Tolmin Basin (Cousin, 1981; Rožič, 2009) and is relatively well studied (e.g., Rožič et al., 2009; Gale, 2010; Gale et al., 2012; Goričan et al., 2012; Rožič et al., 2017, with references). The second basin has been identified on the basis of Upper Triassic to Lower Jurassic open-marine facies exposed in the northern Julian Alps (Lieberman, 1978; De Zanche et al., 2000; Gianolla et al., 2003; Gale et al., 2015), the Southern Kara-

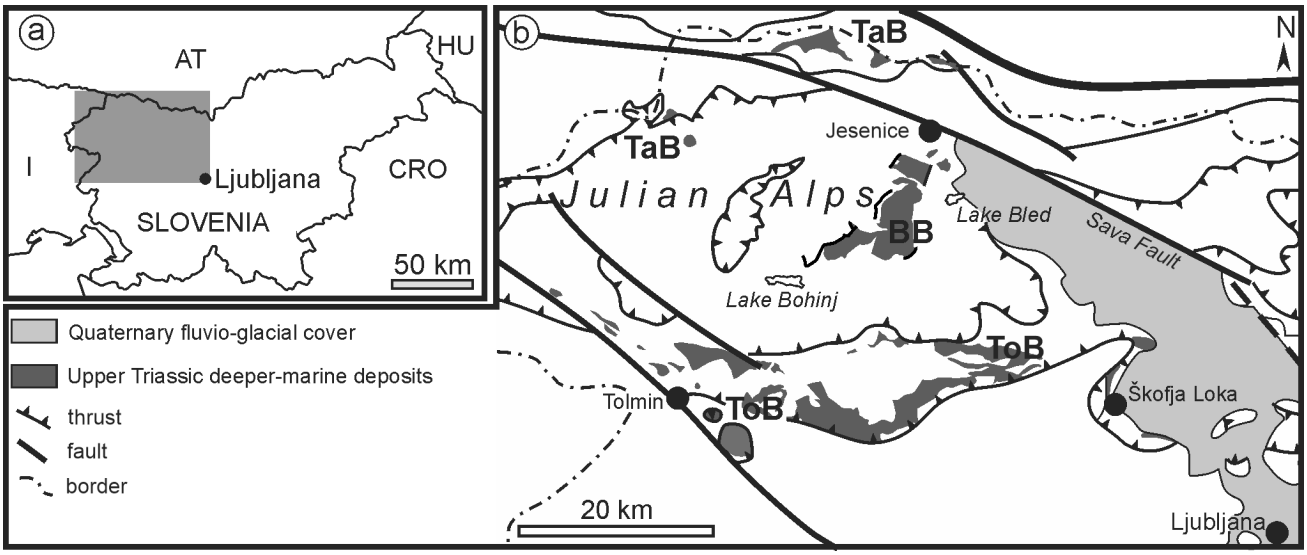


Fig. 1. Location of the studied area. (a) Geographic position of the area shown in Figure 1b. (b) Simplified tectonic map of NW Slovenia with extent of Upper Triassic deeper-marine deposits divided into distinct basins, as discussed in the paper: Bled Basin (BB), Tarvisio Basin (TaB), and Tolmin Basin (ToB). The map is modified after Placer (1999), Buser (2010), Gale et al. (2015), Goričan et al. (2018). The spatial distribution of basinal deposits is based on the map in Rožič (2016).

vanke Mountains (Krystyn et al., 1994; Lein et al., 1995; Schlaf, 1996), and in several outcrops west of this area (Geyer, 1900; Gianolla et al., 1998, 2010; Caggiati, 2014). Gianolla et al. (2010) and Gale et al. (2015) refer to this paleogeographic unit as the Tarvisio Basin. Finally, the third area with Upper Ladinian to Lower Cretaceous deeper marine successions, paleogeographically belonging to the Bled Basin, extends between the lakes Bohinj and Bled (Fig. 1).

The stratigraphic succession of the Bled Basin starts with Upper Anisian – Ladinian carbonate breccias and volcaniclastic rocks deposited on top of massive Anisian dolomite (Buser, 1980). The overlying formation, which constitutes the focus of this paper, is composed of bedded limestone with chert some hundreds of meters thick (Cousin, 1981; Buser, 1987; Goričan et al., 2018). This formation was first noted by Diener (1884), Härtel (1920), and Budkovič (1978). Cousin (1981) referred to it as the Zatrnik Limestone. He considered the upper part of the Zatrnik Limestone to be Rhaetian to Early Jurassic in age, while the base of the formation was dubiously placed in the Carnian. The name Zatrnik Limestone was later abandoned and the informal term Pokljuka Limestone or Pokljuka Formation was more commonly used instead (Dozet & Buser, 2009; Buser, 2010). Fossil bivalves (Buser, 1980) and conodonts (Kolar-Jurkovšek et al., 1983; Ramovš, 1986, 1998), confirmed ages from Late Ladinian to Late Norian, but no continuous sections have

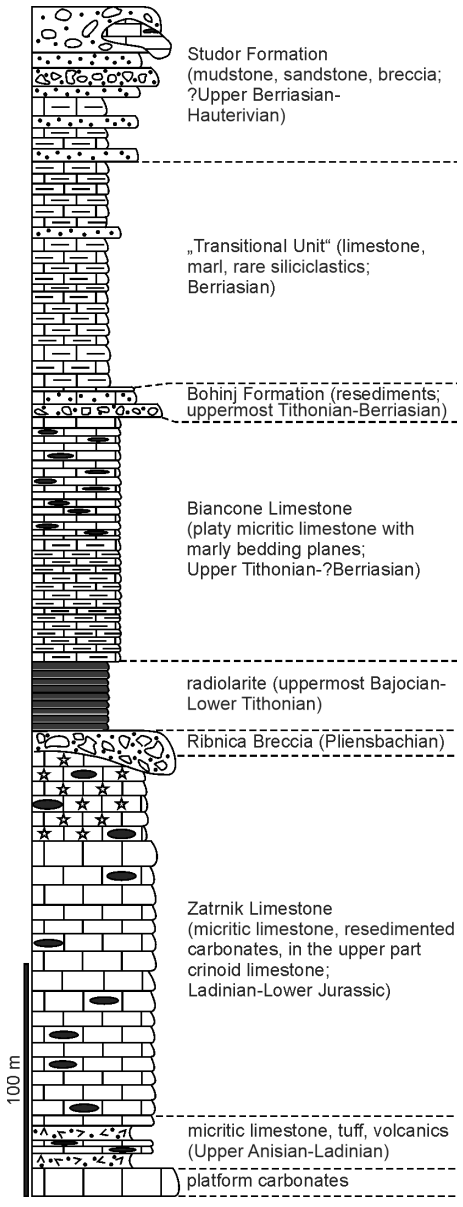


Fig. 2. Lithostratigraphy of the Bled Basin (Pokljuka Nappe). The thickness of the Zatrnik Limestone is not yet fully reconstructed. The measured sections indicate roughly 220 m covering Longobardian to Lower Norian. Modified after Goričan et al. (2018).

been logged. The recent reambulation of the area stratigraphically places the Zatrnik Limestone between the Upper Anisian to Ladinian volcanics and volcaniclastics, and the Pliensbachian carbonate Ribnica Breccia. The succession continues with various pelagic and gravity deposits (see Fig. 2 and Goričan et al., 2018).

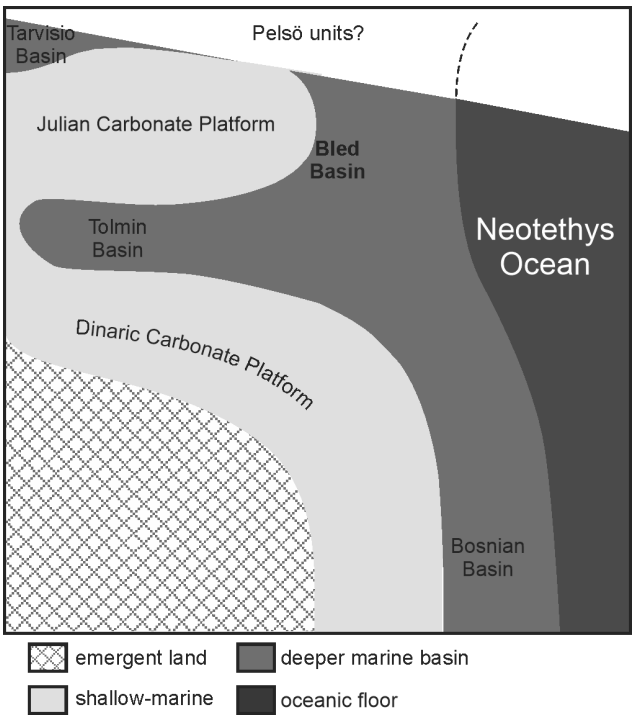


Fig. 3. Paleogeographic position of the Tolmin, Bled and Tarvisio basins at the end of the Carnian. Note that continuations of the units towards the present north are uncertain due to displacements along the Periadriatic Fault System. Modified after Goričan et al. (2018).

In this paper we present three detailed sections and one schematic section from the eastern part of the Pokljuka plateau encompassing the lower part of the Zatrnik Limestone. The sedimentological characteristics of the Zatrnik Limestone are described for the first time in order to identify the depositional environment and the type of sedimentation there. Conodonts, radiolarians, benthic foraminifera and microproblematica were determined from residues and thin sections.

Geological setting

Recent paleogeographic reconstructions place the Bled Basin on the oceanward side of the Julian Carbonate Platform (Fig. 3; Kukoč et al., 2012; Goričan et al., 2018). The sedimentary succession of the Bled Basin is situated today within the Julian Alps that belong to the eastern Southern Alps (Fig. 4; Placer, 1999). Two episodes of thrusting were recognised in the eastern Southern Alps: the latest Cretaceous–Eocene NW-SE striking and SW verging thrusts are overlapped by younger (Oligocene?–Miocene) E-W striking, S-verging thrusts (Doglioni & Siorpaes, 1990; Poli & Zanferarri, 1995; Placer & Čar, 1998). Goričan et al. (2018) called all nappes of the eastern Julian Alps the Julian Nappes. From the bottom to the top these comprise the Krn Nappe, the Slatna Klippe and the Pokljuka Nappe (Fig. 5). Primary thrust contacts are only preserved around the Slatna Klippe. Elsewhere, they were cut and displaced along NE-SW and NW-SE striking faults. Both, the Krn Nappe and the Pokljuka Nappe in

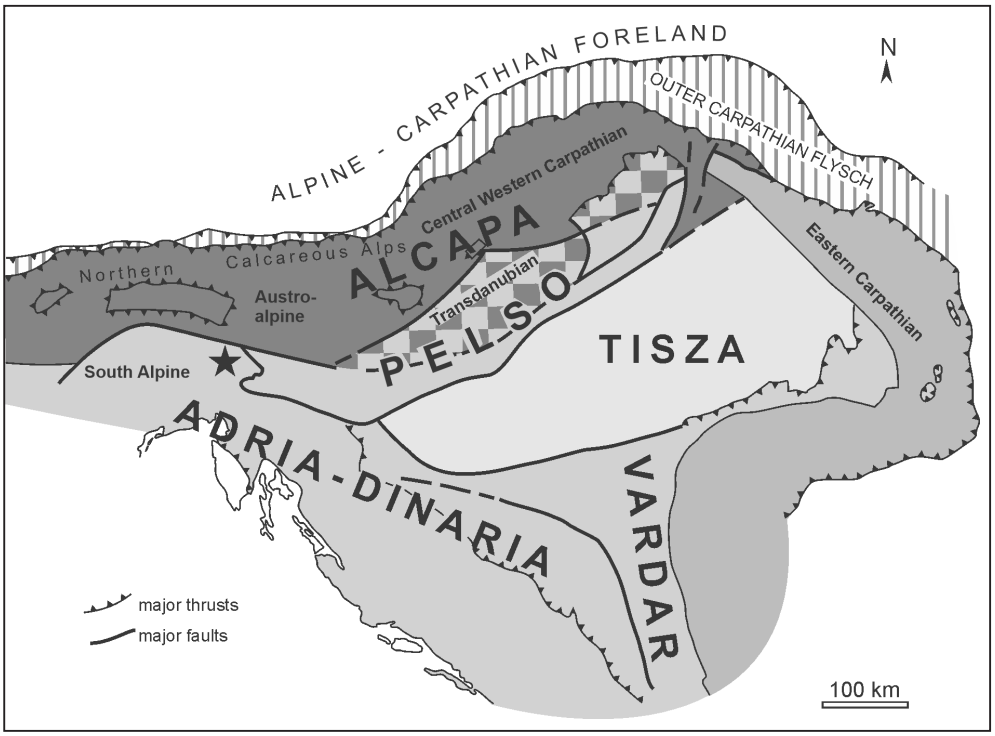


Fig. 4. Position of the studied area (star) on a regional tectonic map. Modified after Kovács et al. (2011).

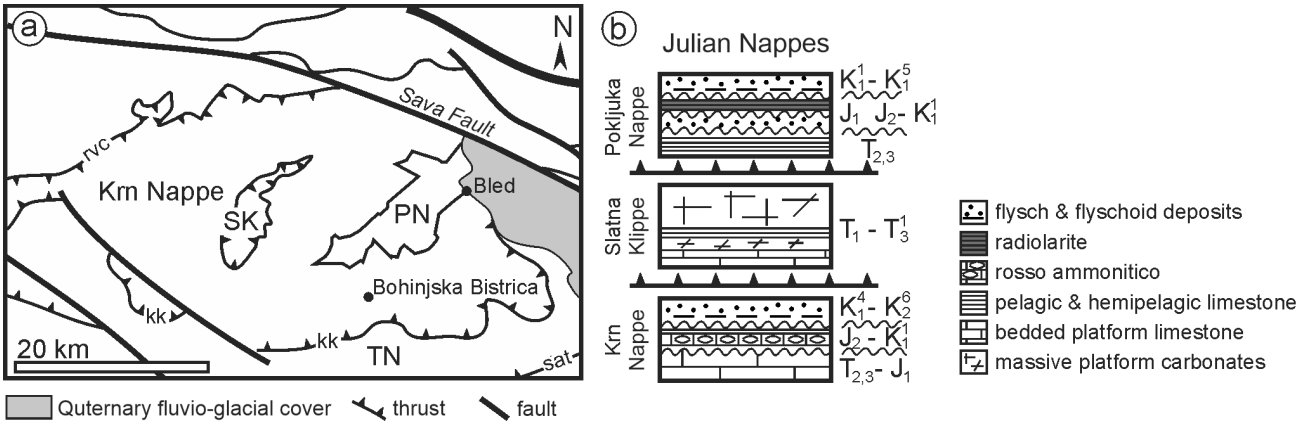


Fig. 5. Structure of the Julian Alps. (a) Schematic structural map of the Julian Alps. Abbrevations: SK – Slatna Klippe, PN – Pokljuka Nappe, TN – Tolmin Nappe, kk – Krn-Kobla Thrust, rvc – Resia-Val Coritenza Backthrust, sat – South Alpine Thrust. Simplified after Gale et al. (2015) and Goričan et al. (2018). (b) Superposition of the Julian Nappes and their simplified lithostratigraphy.

the lower part consist of Anisian shallow marine carbonates and Upper Anisian–Ladinian pelagic limestone and volcaniclastics. In the Krn Nappe and the Slatna Klippe these are followed by massive Carnian limestone and dolomite, while in the Pokljuka Nappe the succession continues with the deeper-marine Zatrnik Limestone (Goričan et al., 2018, with references). Towards the south, the Julian Nappes are in thrust or steep reverse-fault contact with the Tolmin Nappe, preserving successions of the Tolmin Basin (Placer, 1999). The investigated sections within the Zatrnik Limestone were logged in relatively tectonically undisturbed blocks of the Pokljuka Nappe with gently to moderately steep dipping strata, generally in the W and NW directions.

Material and methods

The lowermost part of the Zatrnik Limestone was logged in four sections (Fig. 6). Microfacies analysis is based on 174 thin sections 47×28 mm in size. Thin sections were studied in transmitted light with an optical microscope. Dunham's (1962) classification was used for the description of textures. Point-counting was performed on microphotographs taken from selected thin sections. We counted 300 points on a random grid using JMicroVision v1.2.7 (Copyright 2002-2008 Nicolas Roduit) software. Composite conodont samples were taken over intervals of 1.5 to 10 m, depending on the uniformity of the lithology. Carbonate rock samples were treated in acetic acid (*cca.* 8 %) followed by heavy liquid separation. The recovered faunas are kept in the micropaleontological collection at the Geological Survey of Slovenia (samples GeoZS 5793-5798, 5924-5928, 6001-6019). The SEM photos of conodont specimens were taken at the GeoZS (JEOL JSM

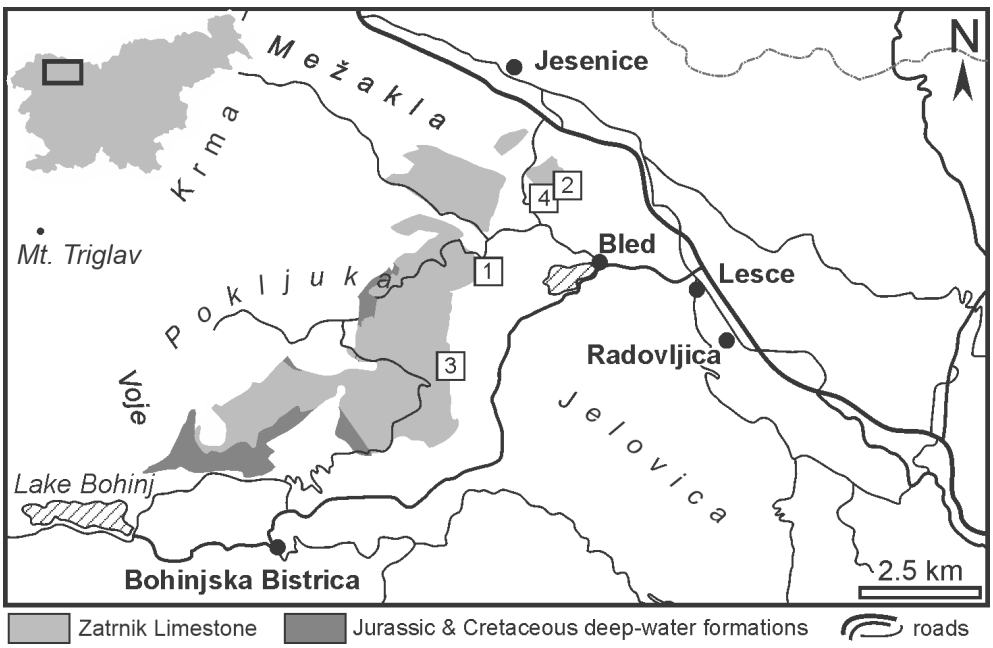


Fig. 6. Geographic position of the studied sections. The numbers indicate sections: Zatrnik (1), Blejski vintgar (2), Galetovec (3), and Poljane (4). Distribution of the basinal formations is drawn after Buser (2009), and Goričan et al. (2018).

6490LV Scanning Electron Microscope). Conodont biostratigraphy follows Rigo et al. (2018), and Kolar-Jurkovšek and Jurkovšek (2019). It should be noted, however, that Chen et al. (2015) have a slightly different view on the species and their ranges, so that stratigraphic boundaries could also be assigned somewhat differently. At the Zatrnik location, two radiolarian samples were taken after radiolarians were detected in the field with a hand lens. These samples were processed in the same manner as the conodont samples. The illustrated radiolarian specimens are stored at ZRC SAZU, Ljubljana (samples RA 5843, RA 5844).

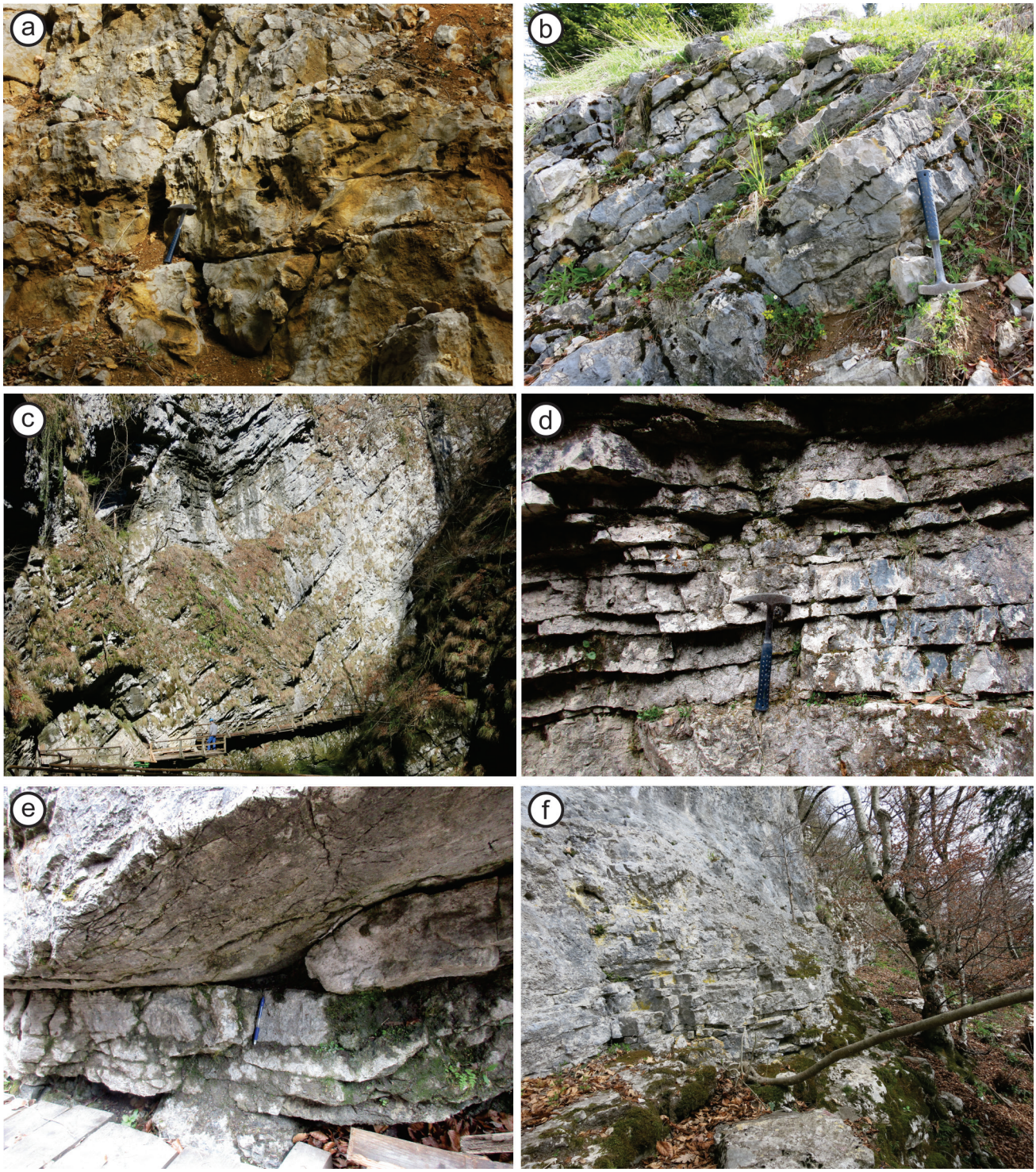


Fig. 7. Field view of the Zatrnik Limestone. **(a)** Medium-thick bedded mudstone with chert nodules, characterizing the upper (Norian and Rhaetian?) part of the formation. **(b)** Zatrnik Limestone at the top of the Zatrnik section, Carnian. **(c)** View of the Blejski vintgar gorge with exposures of the Carnian part of the formation. **(d)** Thin-bedded calcarenites (packstone, grainstone) in the Blejski vintgar section. **(e)** Slump and scour structures in the Blejski vintgar section. **(f)** Transition from bedded limestone with chert into seemingly massive limestone in the Poljane section.

Description of sections

In the lower part the Zatrnik Limestone is represented by thin- and medium-bedded cherty micritic limestone and calcarenites. Medium-thick bedded micritic limestone with chert nodules is the dominant lithofacies in the upper part of the formation (Fig. 7). The logged sections comprise only the lower, Upper Ladinian to Lower Norian part of the formation (Fig. 8), as a good exposure of the Norian and Rhaetian part of the formation has yet to be found. A detailed description of microfacies (MF) types from the logged sections (Figs. 9–12) is given in Table 1 and which are illustrated in Figures 13–14, whereas the determined fossils are listed in Table 2 and illustrated in Figures 15–17.

The Zatrnik section (bottom: 46°21'47''N, 14°2'25''E; top: 46°21'56''N, 14°2'26'' E) is stratigraphically the lowest of the logged sections. Fragments of volcanics and tuff are found in the scree, approximately 10–15 m below the section. Platy to medium-bedded loose bioclastic wackestone (MF 2 in Table 1) predominates (Fig. 9); this limestone may be silicified and locally has small chert nodules. Thin layers of dark brown marlstone intercalate with limestone in the lower 3 m of the formation. Radiolarian fauna (Fig. 16) from two samples of radiolarian packstone (MF 3), taken in this part of the section, indicates Upper Ladinian *Muelleritortis cochleata* Zone (Kozur & Mostler, 1994, 1996). Marlstone is absent in the section higher up. Filament-radiolarian-peloidal packstone (MF 8; Fig. 13c) sporadically intercalates with loose wackestone. Parallel lamination is rarely present. Moving upwards, the proportion of packstone gradually increases. Slumping and amalgamations are locally visible. Conodonts *Gladigondolella malayensis* Nogami, *Budurovignathus* cf. *diebeli* (Kozur & Mock), *B. mostleri* (Kozur) and *Paragondolella praelindae* Kozur suggest that beds above the radiolarian fauna and up to the 24th meter of the section are (middle-late) Julian in age. Between the 26th and 46th meter, the conodont assemblage comprises *P. praelindae*, *Quadralella polygnathiformis* (Budurov & Stefanov) and rare *Q.* aff. *noah* (Hayashi), indicating early-middle Tuvalian age (Rigo et al., 2018; Kolar-Jurkovšek & Jurkovšek, 2019). From the 57th meter up, peloidal packstone (MF 4), peloidal grainstone (MF 9), pebbly intraclastic grainstone (MF 10), bioclastic-intraclastic floatstone (MF 12), and closely-fitted intraclastic rudstone (MF 13) also occur among microfacies types. Normal grading is present in some beds. Approximately 60 m from the base of the section, *P. praelindae* is accompanied by *Paragondolella inclinata* (Kovacs), and later by *Paragondolella tadpole* (Hayashi). The association indicates late Julian to early Tuvalian age. When we also take into consideration the low number of specimens, which makes determination of assemblages difficult, we suggest the sequence between 11th and 24th m of the section is (undivided) Julian in age, while the upper part of the section is early Tuvalian.

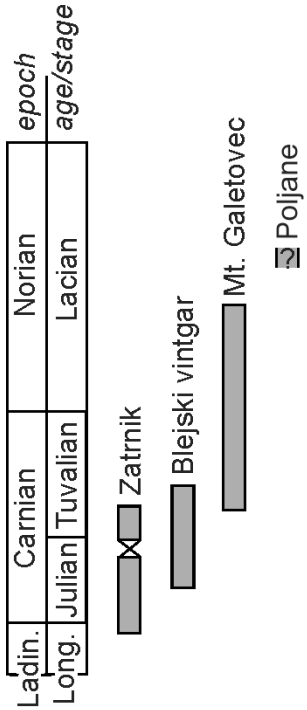


Fig. 8. Schematic position of the logged sections as indicated by biostratigraphic data. The position of the Poljane section is uncertain due to negative conodont samples.

The Blejski vintgar section (bottom: 46°23'49''N, 14°5'19''E; top: 46°23'54''N, 14°5'24''E) was logged in shorter subsections and separated by minor faults (Fig. 10). In contrast to the Zatrnik section, this part of the formation is dominated by pebbly intraclastic grainstone (MF 10). Peloidal grainstone (MF 9) and peloidal-intraclastic packstone (MF 7) are also common, while other microfacies types (MF 2 - loose bioclastic wackestone, MF 4 - peloidal packstone, MF 5 - bioclastic wackestone to packstone, MF 6 - dense mollusc wackestone, MF 8 – filament-radiolarian-peloidal packstone) are subordinate. Scour structures, normal and inverse grading are often observed in micritic limestone, but rarely parallel

Fig. 9. Sedimentary log of the Zatrnik section with ranges of conodont species. Microfacies types (see Table 1) are indicated on the right side of the logs.

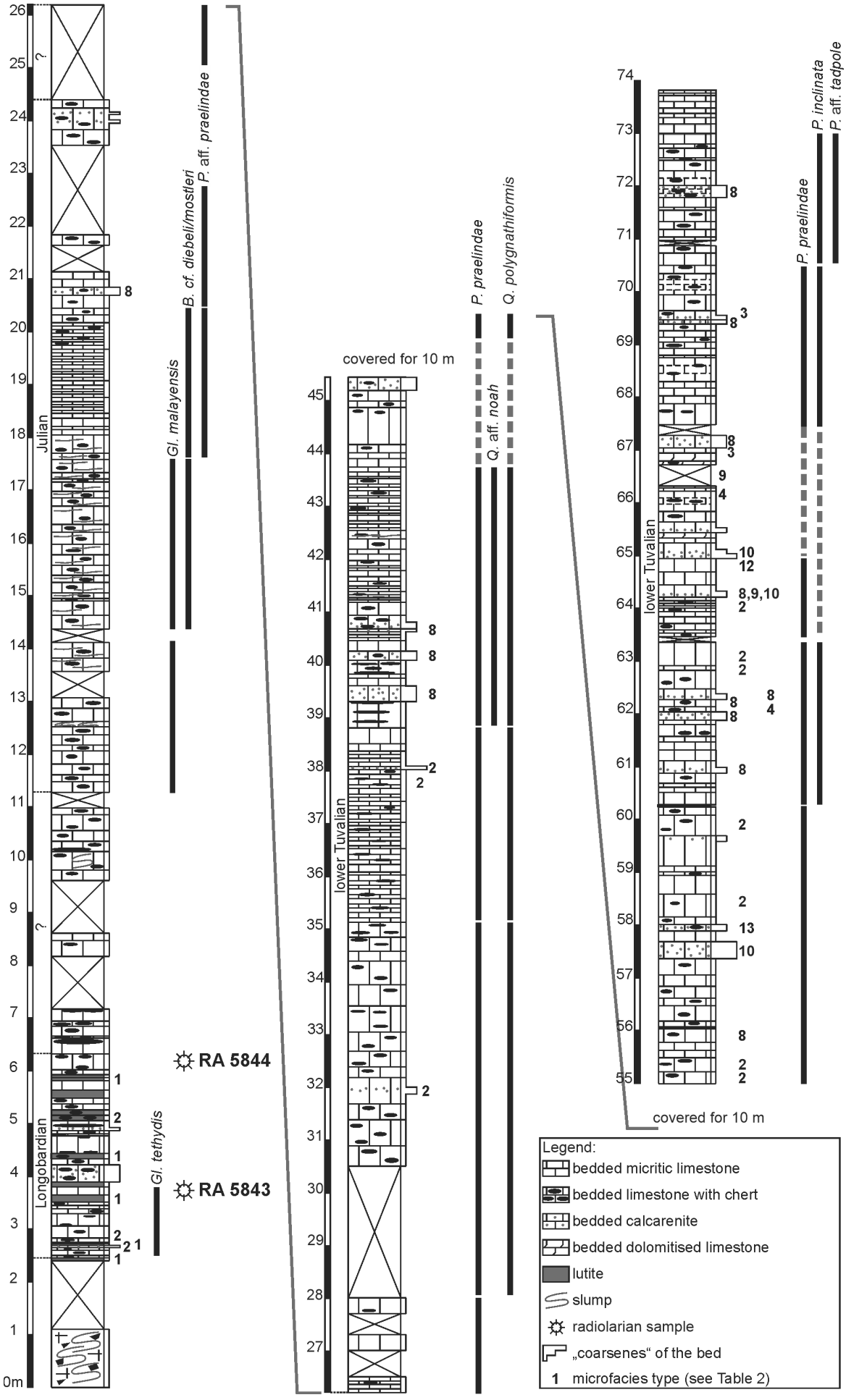

Julian
Longobardian
lower Tuvalian
lower Tuvalian
covered for 10 m
covered for 10 m
Gl. malayensis
B. cf. diebeli/mostleri
P. aff. praelindae
Gl. tethydis
P. praelindae
Q. aff. noah
Q. polygnathiformis
P. praelindae
P. inclinata
P. aff. tadpole
RA 5844
RA 5843
Legend:
bedded micritic limestone
bedded limestone with chert
bedded calcarenite
bedded dolomitised limestone
lutite
slump
radiolarian sample
„coarsenes“ of the bed
1 microfacies type (see Table 2)

Fig. 9.

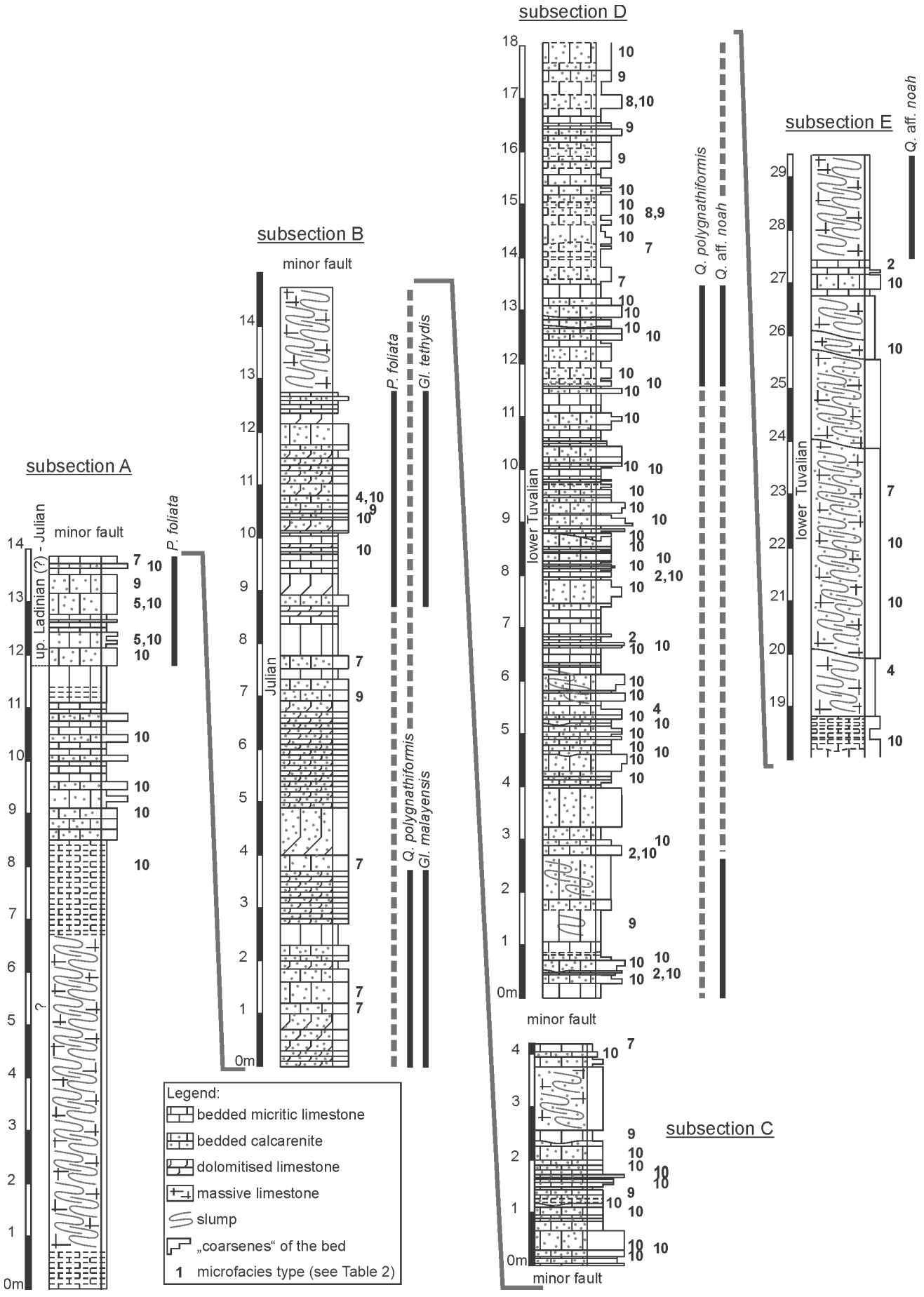


Fig. 10. Sedimentary log of the Blejski vintgar section with ranges of conodont species. Microfacies types (see Table 1) are indicated on the right side of the logs.

lamination and amalgamation. Slumps up to approx. 6 m thick are common. Conodont samples from the lower 12 m of the subsection A were negative. *Paragondolella foliata* Budurov was recovered from the upper 2 m. Subsection B comprises *Paragondolella foliata* Budurov, *Q. polygnathiformis, G. malayensis* and *G. tethydis* (Julian). Subsection D contains *Q. polygnathiformis* and *Q.* aff. *noah,* suggesting early Tuvalian age.

At Mt. Galetovec (bottom: 46°19'38''N, 14°2'28''E, top: 46°19'36''N, 14°2'23''E), the section was measured schematically along the sides of a vertical wall. Micritic limestone with chert nodules predominates (Fig. 11), and the beds tend to thicken towards the top. Amalgamation is commonly present, and some massive beds probably represent slumps. *Quadralella tuvalica* (Mazza & Rigo) was found at the base of the cliff wall, indicating early to middle Tuvalian age (Rigo et al., 2018). In the samples from higher up in the section *Epigondolella quadrata* Orchard, *Epigondolella rigoi* Noyan & Kozur and *Epigondolella vialovi* (Buryi) were collected. The stratigraphic range of all three species originates from the late Tuvalian to the Lacian (Rigo et al., 2018). The upper part of the section also contains some beds of pebbly intraclastic grainstone (MF 10), but in contrast to the same MF type in the Zatrnik and Blejski vintgar sections, the amount of microbialites, microbial-sponge boundstone clasts and microproblematica is clearly lower on account of mollusc fragments. The difference in foraminiferal assemblages is also very obvious: whereas foraminifera are rare, but diverse in the two stratigraphically lower sections, samples from the top of the Mt.Galetovec section commonly contain involutinids *Aulotortus sinuosus* Weynschenk and *Parvalamella friedli* (Kristan-Tollmann), which can be present in relative abundance.

The fourth section was logged at Poljane (46°23'46''N, 14°4›32»E; Fig. 12). Medium, and rarely thick beds of micritic limestone (MF 2 – loose bioclastic wackestone) and fine-grained bioclastic wackestone to packstone (MF 5) are present in the lower part of the section. Amalgamation and chert nodules are locally present. Just as at the top of the Mt. Galetovec section, skeletal carbonate is relatively abundant, and the foraminiferal assemblage is dominated by aulotortids. Thus, we presume these beds are late Tuvalian or younger in age. The section ends at the foot of the massive limestone unit, which is several tens of meters thick. Indistinct, slightly curved and sloping bedding planes can be seen in the lowermost part of this massive limestone

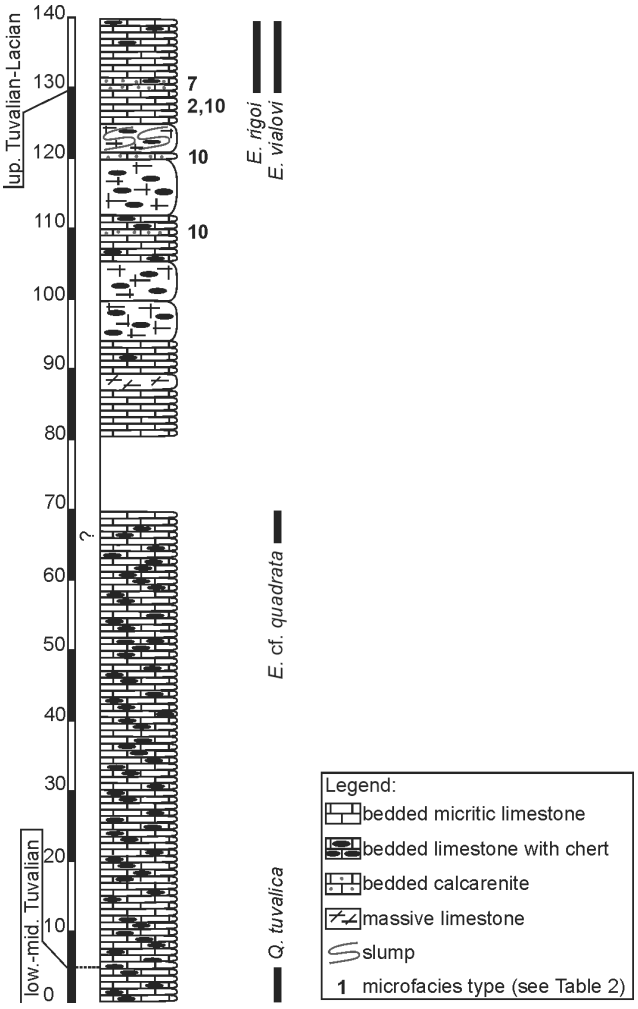


Fig. 11. Sedimentary log of the Mt. Galetovec section with ranges of conodont species. Microfacies types (see Table 1) are indicated on the right side of the logs.

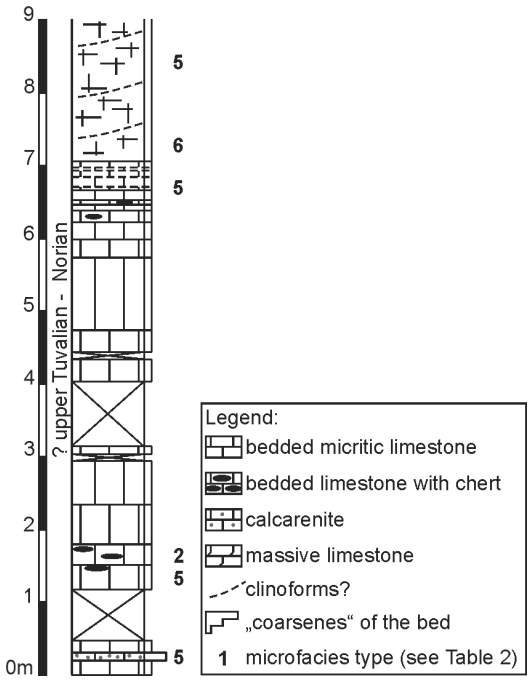


Fig. 12. Sedimentary log of the Poljane section. Microfacies types (see Table 1) are indicated on the right side of the logs.

(see Fig. 7f), texturally a bioclastic wackestone to packstone (MF 5) and a dense mollusc wackestone (MF 6). Foraminifera *Alpinophragmium perforatum* Flügel was found in this part. This species is mostly known from the Norian to Rhaetian (e.g., Flügel, 1967; Matzner, 1986; Kristan-Tollmann, 1990; Gale et al., 2012).

Table 1. Description of microfacies types of the Zatrnik Limestone.

Facies	Microfacies (MF)	Description	Figures
marlstone	marlstone (MF 1)	Dark brown marlstone is finely laminated and partly silicified. It is present only in the lowermost part of the Zatrnik section in beds up to 15 cm thick that interchange with limestone. Lamination is caused by different amounts of organic matter (as opaque bands), orientation of elongated particles and small differences in grain size. Besides very fine-grained matrix, there are a few grains large enough to be identified in thin sections: angular quartz grains and chlorite, small peloids and micritic intraclasts (the largest 0.65 mm in diameter), ostracod shells, echinoderm plates, thin-shelled bivalves and radiolarians.	13a
micritic limestone	loose bioclastic wackestone (MF 2)	Due to variations in clast composition, at least three subtypes were recognised. All have a high amount of matrix in common (77–84 %). In subtype MF 2A, 6 % of the matrix has been washed away. Clasts comprise peloids (12%), sparitic fragments (3 %) and echinoderm plates (1.5 %). Nodosariid foraminifers and radiolarians are very rare. In subtype MF 2B, peloids represent 5.5 % of the area; more common are filaments (4.5 %), and possible radiolarians (2 %), whereas sparitic fragments and undetermined bioclasts occupy 1% of the area, and microproblematica (*Plexoramea gracilis*), foraminifers and echinoderm plates each 0.5 %. In MF 2C, there are no vugs and very few peloids. Clasts are sparitic fragments (5.5–12 %), echinoderms (2.5–6 %), and filaments (3.5–5 %).	13b-d
	radiolarian packstone (MF 3)	Radiolarians are in rock-forming abundance, packed closely together. Very rare are thin-shelled bivalves ("filaments"). Radiolarian tests are filled with calcite or are silicified.	13e
	peloidal packstone (MF 4)	Sediment was bioturbated or deposited in laminae 1 cm thick. Average grain size is between 0.06 and 0.07 mm, with the largest grains 0.17 mm in size. Sediment is thus well to very well sorted. Peloids represent around 44 % of the area. Far more rare are fragmented bioclasts replaced by spar (up to 3.5 %), thin-shelled bivalves (3 %), echinoderms, foraminifers (*Agathammina austroalpina*, *Earlandia gracilis*, ?*Hoyenella* sp., *Turriglomina mesotriassica*, nodosariid lagenida), and microproblematica (*Ladinella porata*, *Thaumatoporella parvovesiculifera*, *Tubiphytes*-like form).	13f
	bioclastic wackestone to packstone (MF 5)	Micritic matrix represents 40–61 % of the area; up to 4.5 % of the surface consists of irregular vugs filled with drusy-mosaic spar, possibly representing areas where micrite had been washed away. The composition of clasts is variable, but a few types dominate: peloids (7–15 % of area), micritic intraclasts (up to 17 %; radiolarians were recognised in one), sparitic fragments (3.5–15 %), echinoderm plates (1–15 %) and thin-shelled bivalves (up to 16 %). Foraminifers (*Duotaxis*, sessile forms, and small nodosariid and miliolid species), spicules and ostracods are very rare. One sample contains larger pieces of brachiopod shells.	13g
	dense mollusc wackestone (MF 6)	Grains represent 42 % of the area, and on average measure 0.18 mm in size. Grains are well sorted. Angular sparitic fragments predominate (21 % of the area). Other grains are angular micritic intraclasts (6 %), foraminifers, echinoderm plates, ostracods and thin-shelled bivalves.	13h
calcarenite	peloidal-intraclastic packstone (MF 7)	In most samples, intergranular space is filled with micritic matrix. In fewer samples, most of the mud has been washed away and the space filled by calcitic cement. Grains represent more than 50 % of the thin section area. Average grain size is from 0.1 to 0.2 mm, with the largest grains up to 2 mm. Sorting ranges from moderately to well sorted. The majority of grains are peloids and dark intraclasts, together representing from 20 to 55 % of the thin section area. The latter may be mud chips or fragments of microbialites (distinction is rarely possible at smaller magnifications). Other grains are mostly microproblematica (2.5–4.5 %), echinoderm plates (3–8 %), locally thin-shelled bivalves (up to 11 %), very rare nodosariid foraminifers and brachiopods. Differentiation from MF 4 is by virtue of smaller grain size and better sorting of the latter. Dolomitization is locally present.	14a
	filament-radiolarian-peloidal packstone (MF 8)	Sediment may be laminated, with laminae differing in grain size, density and percentage of thin-shelled bivalves (these are oriented parallel to laminae) and radiolarians. Alternatively, it is bioturbated. Grains represent 65–70 % of the area. Peloids measure 0.07–0.09 mm (largest up to 0.24 mm), while radiolarians measure 0.18–0.20 mm in size. Intraclasts, although rare, are the largest grains with diameters of up to 6 mm. Peloids are thus very well sorted. The upper-size limit is represented by light echinoderm plates and flat thin-shelled bivalves. The most common grains are peloids (26–37 %), thin-shelled bivalves (9.5–34 %), radiolarians (2.5–25 %) and echinoderms (3.5–7.5 %). Intraclasts represent 0.5–1 % of the area, while foraminifers, sparitic clasts, ostracods, fragments of brachiopods, microproblematica and possible dasycladacean algae are very rare. Intergranular space is filled with micritic matrix, locally recrystallized into pseudosparite. Larger calcite crystals fill the space beneath bivalves. Echinoderm plates are overgrown by syntaxial calcite cement.	14b
	peloidal grainstone (MF 9)	Sediment is locally horizontally laminated (laminae differ in grain size, or exchange with laminae of other MF type). Grains represent approximately 70 % of the area; intergranular space is filled by granular or drusy-mosaic calcite spar. Grains on average measure 0.15 mm, while the largest reach 0.83 mm in size. Sediment is moderately well to well sorted. Peloids are the predominating grain type (50–60 %). Also present are sparitic fragments (6.5–9 %), echinoderm plates (1.5–2.5 %), microproblematica (up to 4.5 %). Foraminifera, gastropods, calcimicrobes and brachiopod fragments are very rare. Echinoderm plates are overgrown by syntaxial calcite. Dolomitization is locally present; dolomite crystals are euhedral, overgrowing peloids or crosscutting older cement and grains.	14c
	pebbly intraclastic grainstone (MF 10)	Grading is commonly present. The largest clasts measure up to 1 cm in size, while average grain size is 0.3 to 0.5 mm (size changes with grading). Grains are angular and in point contacts. They comprise between 45–75 % of the area (on average 67 %). The most common grains are intraclasts (49.5 %). Microproblematica is more common in Ladinian and Carnian samples (7.5 % compared to 0.5 % in the Norian samples; note that this is a very conservative estimate, as point counting was performed mainly at small magnifications, which often do not allow for differentiation from micritic intraclasts). Sparitic fragments (5.9 %), echinoderms (3.4 %), and foraminifers (1 %) appear in approximately the same abundance, irrespective of the samples' age.	14d-e

	pebbly intraclastic grainstone (MF 10)	**Within the lower – middle Carnian part** of the succession, intraclasts comprise pelletal packstone with *Bacinella floriformis*, peloidal packstone, bioclastic-peloidal packstone, bioclastic wackestone, calcimicrobes (types *Garwoodia* and *Cayeuxia*), microproblematica-sponge boundstone, microbialite (stromatolite, pelletal leiolite), *Bacinella*-like boundstone clasts and cementstone. Other clasts are peloids (small intraclasts), sparitic fragments, microproblematica, echinoderm plates, foraminifers, radial spherulites, brachiopods, rare green algae, agglutinated worm tubes, bryozoan and ammonite fragments, gastropods and ostracods. **In the upper Carnian – lower Norian samples**, mudstone, mudstone with filaments and spicules and calcimicrobes are present among intraclasts, whereas smaller grains contain peloids (small micritic intraclasts), echinoderms, foraminifers, spherulites, sparitic fragments (cortoids), agglutinated worm tubes, and brachiopod fragments. Besides fewer (or even the absence of) microbialites, microbial-sponge boundstones and microproblematica, Carnian and Norian samples differ notably in foraminiferal assemblage. Cement is represented by drusy mosaic calcite. Fibrous rim cement occurs locally. In some samples, coarse euhedral dolomite fills the intergranular space. Only one example of silicified valves was found.	14d-e
	intraclastic-mollusc packstone (MF 11)	Grains represent approximately 70 % of the area. The intergranular space is filled with micritic matrix (27 % of the area) and drusy mosaic calcite cement (4 %). Grains are mostly in point contacts. Sorting is medium to poor, with the average size of grains around 0.35 mm and the largest grains measuring 2 mm in size. The most abundant grains are sparitic fragments (31 % of the area). Most are probably mollusc fragments, but some may belong also to recrystallized involutinid foraminifers. Intraclasts (bioclastic wackestone and packstone) occupy another 23 % of the area. Other grains are echinoderm plates (11.5 %), foraminifers (3 %), small fragments of *Thaumatoporella* thalli, and ostracods. Some grains are selectively silicified.	14f
fine-grained breccia	bioclastic-intraclastic floatstone (MF 12)	Micritic matrix represents 46 % of the area, whereas clasts occupy the rest of the space. Clasts are poorly sorted, up to 4.5 mm large. Among them, intraclasts are the most common (23 % of area). They are variable, mostly angular, comprising bioclastic-peloidal wackestone, cementstone, mudstone (or structureless microbialite), stromatolite, microproblematica boundstone, and *Bacanella* boundstone. Other clasts include fragments of bivalves, oncoids, microproblematica (*Tubiphytes*, *Plexoramea*, *Ladinella*), *Dendronella* algae, sponges, echinoderm plates, foraminifers, solitary corals, gastropods and ostracods. Bivalve shells are micritized at the margins. Aragonite is replaced by drusy mosaic calcite.	14g
	closely-fitted intraclastic rudstone (MF 13)	One sample comprises closely fitted angular intraclasts (pelletal packstone, fine-grained dense bioclastic-pelletal wackestone, undetermined silicified clasts, bioclastic-intraclastic wackestone). Rare echinoid spines also occur. The matrix between clasts seems to be micritic. Bioclastic-intraclastic grainstone is locally visible among clasts, and may be infiltrated into rudstone.	14h

Table 2. List of determined fossils. Distribution of conodont taxa (from composite samples) is shown next to sedimentary logs in Figures 9–11. See Figure 9 for position of the radiolarian samples.

Fossil group	Taxa
Conodonts	*Budurovignathus* cf. *B. diebeli* (Kozur & Mock) vel *mostleri* (Kozur), *Epigondolella quadrata* Orchard, *E. rigoi* Noyan & Kozur, *E. vialovi* (Buryi), *Gladigondolella tethydis* (Huckriede), *G. malayensis* Nogami, *Paragondolella praelindae* Kozur, *P. foliata* Budurov, *P. inclinata* (Kovacs), *P.* aff. *tadpole* (Hayashi), *Quadralella polygnathiformis* (Budurov & Stefanov), *Q. noah* (Hayashi), *Q. tuvalica* (Mazza & Rigo) **(for distribution of taxa see Figs. 9-12)**
Radiolarians	**Sample 5843 (Zatrnik):** *Acanthotetrapaurinella variabilis* Kozur & Mostler, *Annulotriassocampe* cf. *eoladinica* Kozur & Mostler, *Archaeocenosphaera* sp., *Dumitricasphaera trialata* Tekin & Mostler, *Karnospongella bispinosa* Kozur & Mostler, *Muelleritortis cochleata* (Nakaseko & Nishimura), *M. expansa* Kozur & Mostler, *M.s* aff. *expansa* Kozur & Mostler, *M. longispinosa* Kozur, *M. tumidospina* Kozur, *Paurinella triangularis* Kozur & Mostler, *Pseudostylosphaera nazarovi* (Kozur & Mostler), *Ropanaella* sp., *Scutispongus latus* Kozur & Mostler, *Spinotriassocampe longobardica* Kozur & Mostler, *Spongoserrula rarauana* Dumitrica, *Spongotortilispinus tortilis* Kozur & Mostler, *Triassocampe*? sp., *Tritortis dispiralis* (Bragin) **Sample 5844 (Zatrnik):** *Acanthotetrapaurinella variabilis* Kozur & Mostler, *Archaeocenosphaera* sp., *Dumitricasphaera trialata* Tekin & Mostler, *Muelleritortis cochleata* (Nakaseko & Nishimura), *M. expansa* Kozur & Mostler, *Paurinella triangularis* Kozur & Mostler, *Pseudostylosphaera nazarovi* (Kozur & Mostler), *Ropanaella* sp., *Scutispongus latus* Kozur & Mostler, *Spongoserrula rarauana* Dumitrica, *Spongotortilispinus slovenicus* (Kolar-Jurkovšek), *Steigerispongus cristagalli* (Dumitrica), *Triassocampe*? sp., *Tritortis dispiralis* (Bragin)
Foraminifera	**Carnian (Zatrnik and Blejski vintgar sections, lower part of Galetovec sections):** *Glomospirella* cf. *pokornyi* (Salaj), *Reophax rudis* Kristan-Tollmann, *Ammobaculites* sp., *Gaudyina* sp., *Paleolituonella meridionalis* (Luperto), *Earlandia amplimuralis* (Pantić), *Earlandia tintinniformis* (Mišik), *Agathammina austroalpina* Kristan-Tollmann & Tollmann, *Arenovidalina*/*Ophthalmidium* sp., *Gsollbergella spiroloculiformis* (Oravecz-Scheffer), *Turriglomina mesotriasica* (Koehn-Zaninetti), *Hydrania dulloi* Senowbari-Daryan, *Piallina bronnimanni* Martini et al., *Cucurbita longicollum* Senowbari-Daryan, *C. infundibuliforme* Jablonský, *C.* cf. *minima* Senowbari-Daryan, *Trocholina turris* Frentzen, *Trocholina* sp., Duostominidae, *Koskinobullina socialis* Cherchi & Schroeder, *Pseudonodosaria* cf. *obconica* (Reuss), *Austrocolomia* sp., nodosariid Lagenida **Upper Tuvalian - Lower Norian (middle and upper part of the Galetovec section, Poljane section):** *Pilammina sulawesiana* Martini et al., *Reophax rudis* Kristan-Tollmann, *Ammobaculites* sp., "*Trochammina*" *almtalensis* Koehn-Zaninetti, *Duotaxis* sp., "*Tetrataxis*" *humilis* Kristan, *Alpinophragmium perforatum* Flügel, Endothyracea, *Planiinvoluta* sp., *Agathammina austroalpina* Kristan-Tollmann & Tollmann, *Miliolechina stellata* Zaninetti et al., *Aulotortus sinuosus* Weynschenk, *Parvalamella friedli* (Kristan-Tollmann), Duostominidae, *Variostoma cochlea* Kristan-Tollmann, *Lenticulina* sp., *Pseudonodosaria* sp., nodosariid Lagenida
Microproblematica	**Carnian (Zatrnik and Blejski vintgar sections, lower part of Galetovec sections):** *Tubiphytes* group (?*Tubiphytes obscurus* Maslov), *Plexoramea cerebriformis* Mello, *Ladinella porata* Ott, *Baccanella floriformis* Pantić, *Plexoramea gracilis* (Schäfer & Senowbari-Daryan), *Bacinella irregularis* Radoičić, *Radiomura cautica* Senowbari-Daryan & Schäfer **Upper Tuvalian - Lower Norian (middle and upper part of the Galetovec section, Poljane section):** *Thaumatoporella* sp., ?*Plexoramea cerebriformis* Mello, *Baccanella floriformis* Pantić

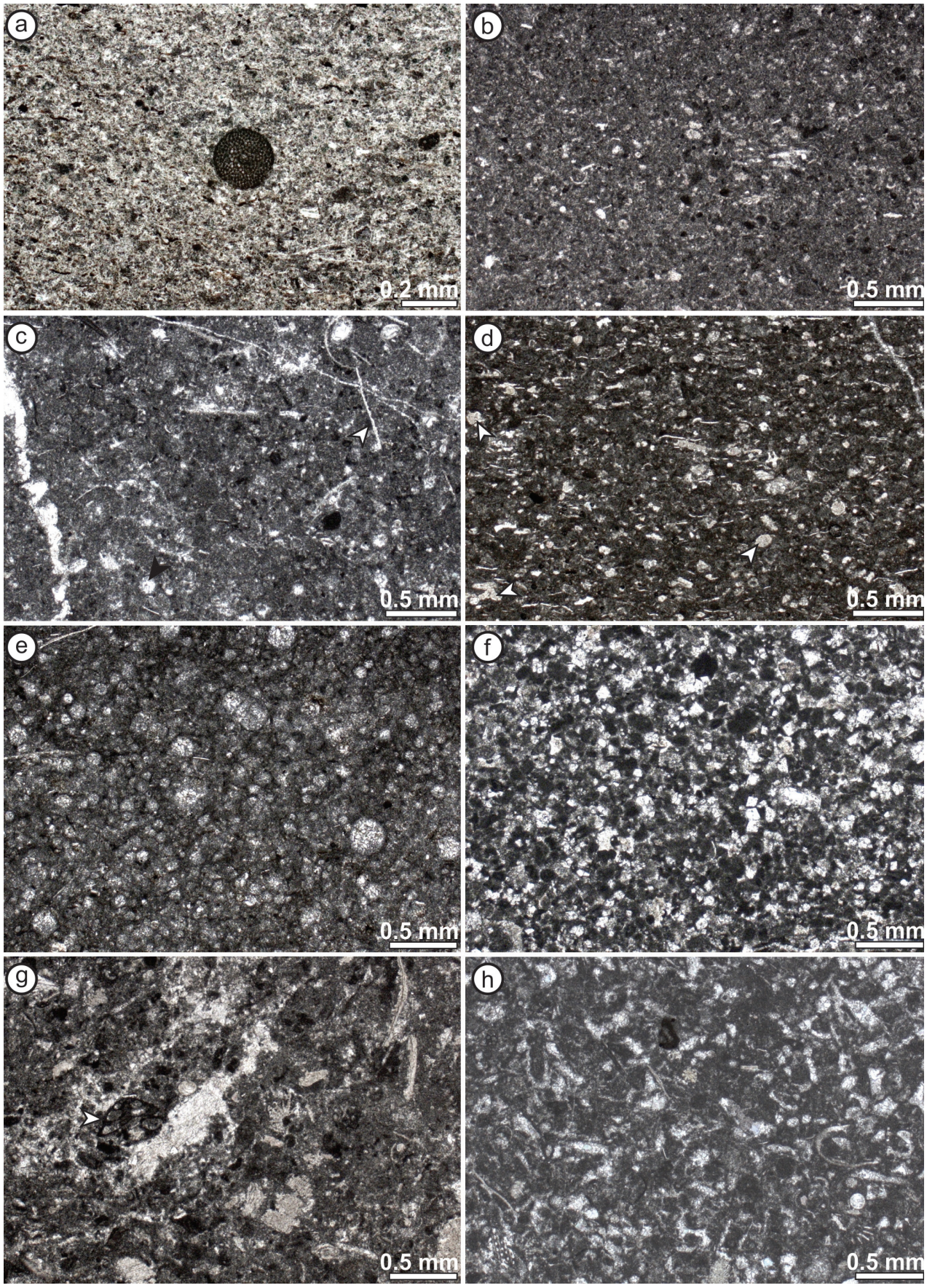


Fig. 13. Microfacies of the Zatrnik Limestone. **(a)** Pyritized (?) radiolarian test in lutite (MF 1). Section Zatrnik; 6th meter. **(b)** Loose bioclastic wackestone (MF 2A). Section Zatrnik; 55th meter. **(c)** Loose bioclastic wackestone (MF 2B). Note rare filaments (white arrowhead) and radiolarians (black arrowhead). Section Zatrnik; 32nd meter. **(d)** Loose bioclastic wackestone (MF 2C). Note slightly greater abundance of echinoderms (arrowhead). Section Zatrnik; 60th meter. **(e)** Radiolarian packstone (MF 3). Section Zatrnik; 4th meter. **(f)** Peloidal packstone (MF 4), slightly dolomitized. Blejski vintgar section, subsection D; 5.5 meters. **(g)** Bioclastic wackestone to packstone (MF 5). Note foraminifera *Duotaxis* sp. (arrowhead). Section Poljane; 1.2 meters **(h)** Dense mollusc wackestone (MF 6). Section Poljane; 6.5 meters.

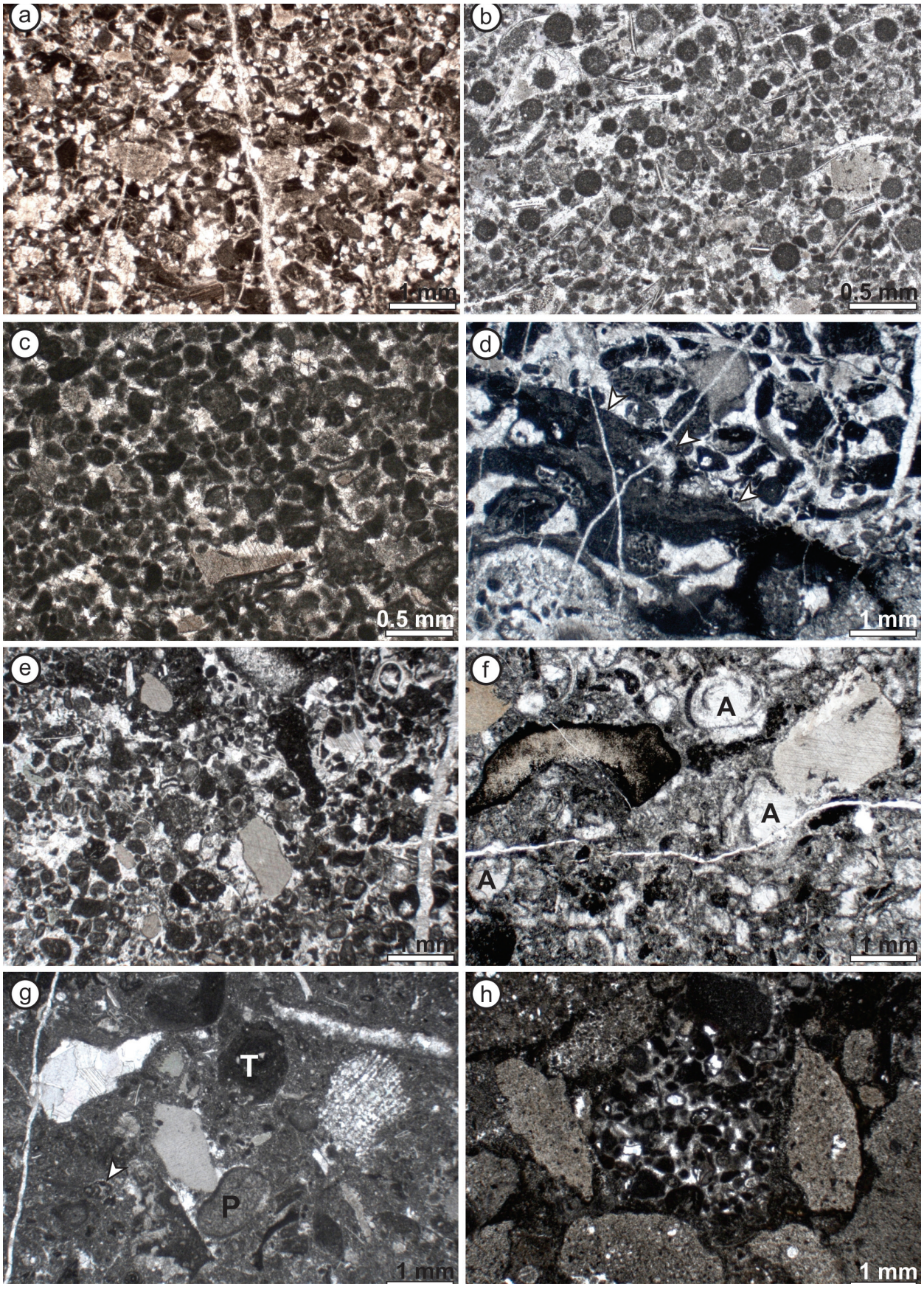


Fig. 14. Microfacies of the Zatrnik Limestone. **(a)** Peloidal-intraclastic packstone (MF 7). Section Blejski vintgar; subsection B; 1st meter. **(b)** Filament-radiolarian-peloidal packstone (MF 8). Section Zatrnik; 69.5 meters. **(c)** Peloidal grainstone (MF 9). Section Blejski vintgar, subsection D; 16.5 meters. **(d)** Pebbly intraclastic grainstone (MF 10). Arrowheads point at the margin of the microbialite boundstone. Section Blejski vintgar, subsection A; 10.5 meters. **(e)** Pebbly intraclastic grainstone (MF 10). Sample 1177. **(f)** Intraclastic-mollusc packstone (MF 11). Section Galetovec; 110th meter. Letter "A" denotes foraminifera *Parvalamella friedli* (Kristan-Tollmann). **(g)** Bioclastic-intraclastic floatstone (MF 12). Letter "T" denotes *Tubiphytes*-like clast, letter "P" a *Plexoramea*, and white arrowhead a small foraminifera *Reophax* sp. Section Zatrnik; 58.5 meters. **(h)** Closely-fitted intraclastic rudstone (MF 13). Section Zatrnik; 58th meter.

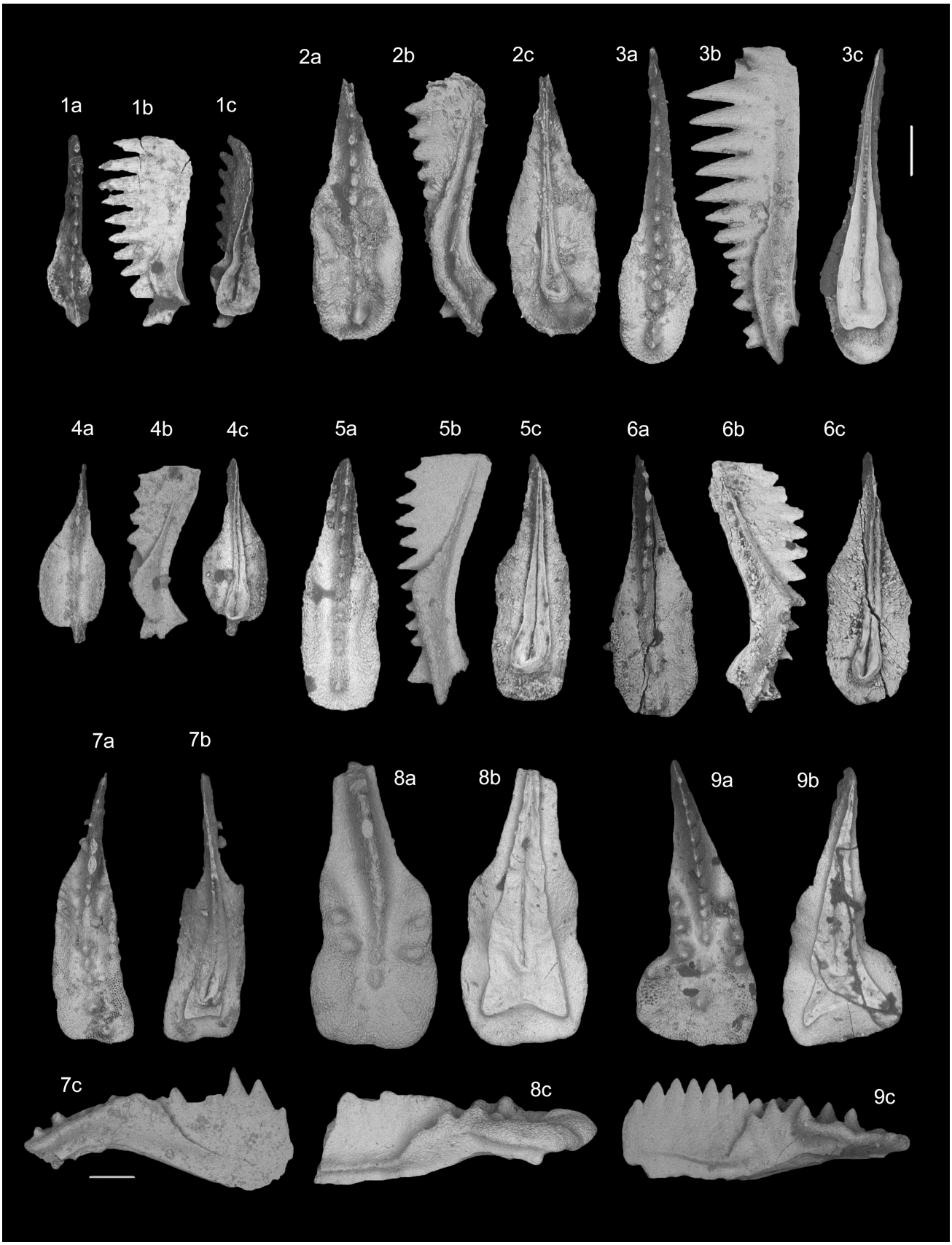


Fig. 15. Conodonts from Late Ladinian to Norian part of the Zatrnik Limestone. **1.** *Paragondolella foliata* Budurov – immature specimens with very wide basal cavity. Sample GeoZS 5793; Blejski vintgar; Julian. **2.** *Paragondolella inclinata* (Kovacs). Sample HV 6006-2; Zatrnik; Julian. **3.** *Paragondolella tadpole* (Hayashi). Sample HV 6006-1; Zatrnik; Julian. **4.** *Paragondolella praelindae* Kozur. Sample ZA 6017-2; Zatrnik; Julian. **5.** *Quadralella polygnathiformis* (Budurov and Stefanov). Sample ZA 6018-1; Zatrnik; Julian. **6.** *Quadralella polygnathiformis* (Budurov and Stefanov) – with rounded posterior and rounded keel. Sample GeoZS 5796; Blejski vintgar; Julian. **7.** *Quadralella tuvalica* (Mazza and Rigo) – primitive form with weak nodes. Sample GA 5928-1; Galetovec; Tuvalian. **8.** *Epigondolella* cf. *quadrata* Orchard. Sample GA 5927-1; Galetovec; Tuvalian-Lacian. **9.** *Epigondolella rigoi* Noyan and Kozur. Sample GA 5924-6; Galetovec; Tuvalian-Lacian.

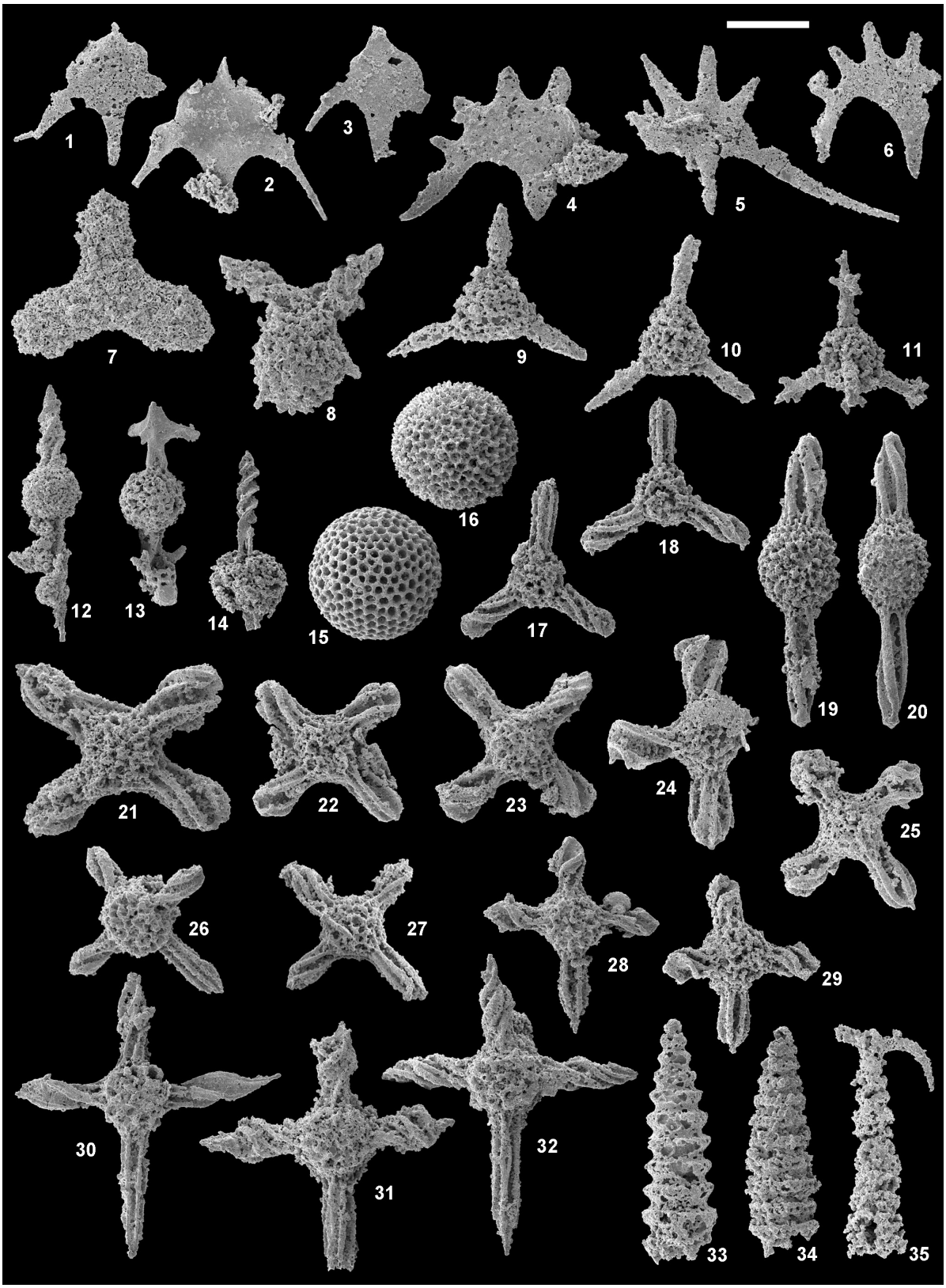


Fig. 16. Late Ladinian radiolarians from locality Zatrnik. **1–3**. *Scutispongus latus* Kozur and Mostler. **4, 6**. *Spongoserrula rarauana* Dumitrica. **5**. *Steigerispongus cristagalli* (Dumitrica). **7**. *Ropanaella* sp. **8**. *Karnospongella bispinosa* Kozur and Mostler. **9–10**. *Paurinella triangularis* Kozur and Mostler. **11**. *Acanthotetrapaurinella variabilis* Kozur and Mostler. **12**. *Spongotortilispinus slovenicus* (Kolar-Jurkovšek). **13**. *Dumitricasphaera trialata* Tekin and Mostler. **14**. *Spongotortilispinus tortilis* Kozur and Mostler. **15–16**. *Archaeocenosphaera* sp. **17–18**. *Tritortis dispiralis* (Bragin). **19–20**. *Pseudostylosphaera nazarovi* (Kozur and Mostler). **21–25, 29**. *Muelleritortis expansa* Kozur and Mostler. **26–27**. *Muelleritortis tumidospina* Kozur. **28**. *Muelleritortis* aff. *expansa* Kozur and Mostler. This species differs from typical *M. expansa* by having pyramidal (not blunt) spine tips on the three torsioned spines and by the fourth spine being slightly longer than the other three. It is also close to *Muelleritortis koeveskalensis* Kozur but typical *M. koeveskalensis* (see the holotype in Kozur, 1988) has sinistrally torsioned spines. **30**. *Muelleritortis longispinosa* Kozur. **31–32**. *Muelleritortis cochleata* (Nakaseko and Nishimura). **33**. *Triassocampe*? sp. **34**. *Annulotriassocampe* cf. *eoladinica* Kozur and Mostler. **35**. *Spinotriassocampe longobardica* Kozur and Mostler.

Sample RA 5843: figs. 2–3, 7–8, 10–11, 13–17, 19, 22–23, 25–31, 33–35. Sample RA 5844: figs. 1, 4–6, 9, 12, 18, 20–21, 24, 32. Length of scale bar 100 µm for figs. 8–11 and 33–35; 150 µm for figs. 1–6, 13–18 and 21–32; 200 µm for figs. 7, 12, 19–20.

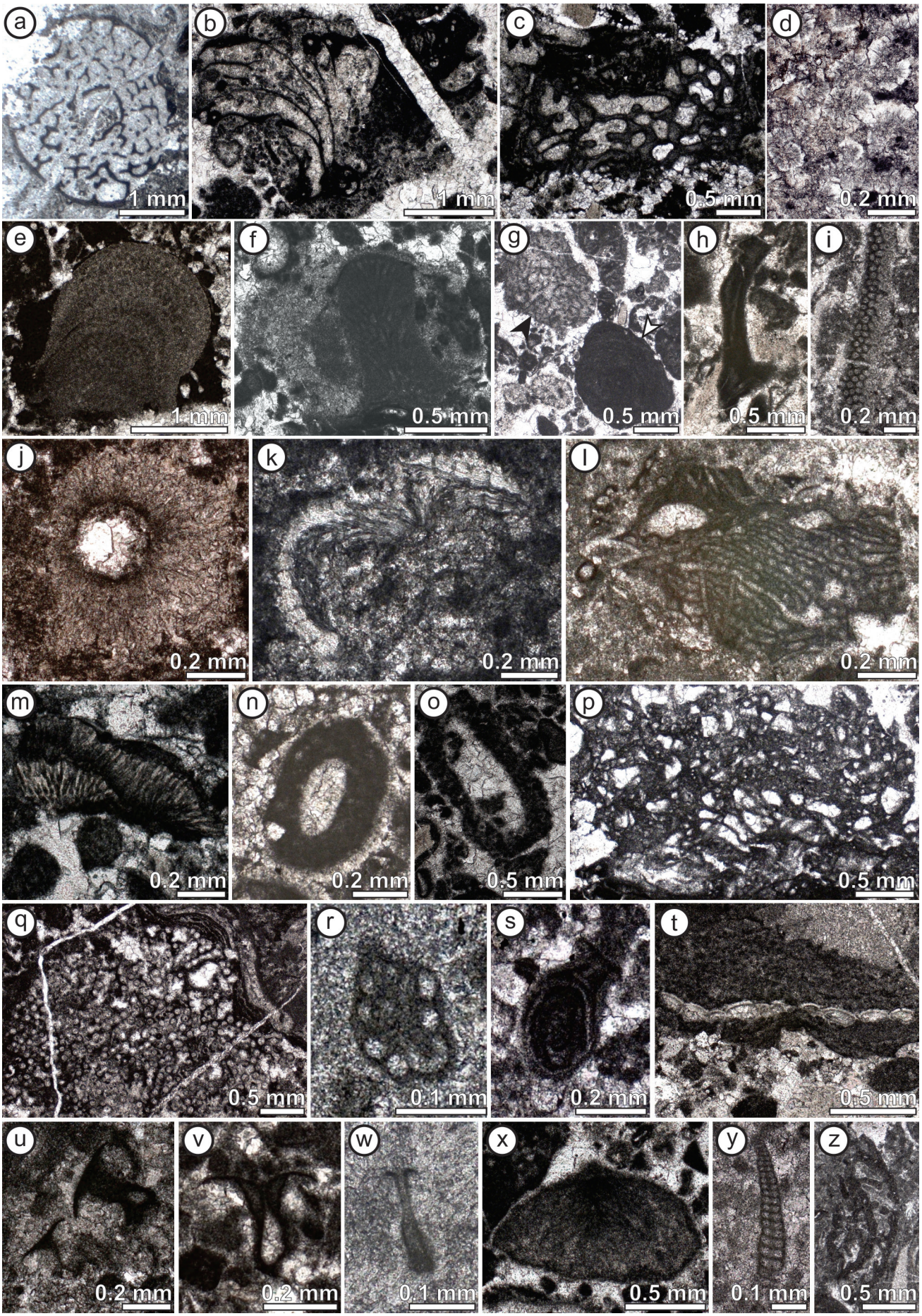

a
1 mm
b
1 mm
c
0.5 mm
d
0.2 mm
e
1 mm
f
0.5 mm
g
0.5 mm
h
0.5 mm
i
0.2 mm
j
0.2 mm
k
0.2 mm
l
0.2 mm
m
0.2 mm
n
0.2 mm
o
0.5 mm
p
0.5 mm
q
0.5 mm
r
0.1 mm
s
0.2 mm
t
0.5 mm
u
0.2 mm
v
0.2 mm
w
0.1 mm
x
0.5 mm
y
0.1 mm
z
0.5 mm

Fig. 17

Fig. 17. Sponges and various microfossils from the Carnian and Norian part of the Zatrnik Limestone. **(a-c)** Undetermined "sphinctozoan" sponges; section Blejski vintgar. (a) Julian. (b-c) Lower Tuvalian. **(d)** *Baccanella floriformis* Pantić; section Blejski vintgar; lower Tuvalian. **(e-f)** *Ladinella porata* Ott; section Blejski vintgar; Julian. **(g)** ?*Tubiphytes obscurus* Maslov (white arrowhead) and *Plexoramea cerebriformis* Mello (black arrowhead); section Blejski vintgar; Julian. **(h)** *Plexoramea gracilis* (Schäfer and Senowbari-Daryan); section Blejski vintgar; lower Tuvalian. **(i)** *Thaumatoporella* sp.; section Poljane; upper Tuvalian? - Lower Norian. **(j-k)** *Radiomura cautica* Senowbari-Daryan and Schäfer; section Blejski vintgar; lower Tuvalian. (j) Transverse section. (k) Longitudinal section. **(l)** Red algae?; section Blejski vintgar; lower Tuvalian. **(m)** Calcimicrobe?; section Blejski vintgar; lower Tuvalian. **(n)** Agglutinated worm tube; section Blejski vintgar; Carnian. **(o)** Agglutinated worm tube (*Terebella* sp.); section Blejski vintgar; lower Tuvalian. **(p)** *Bacinella irregularis* Radoičić; section Blejski vintgar; Carnian. **(q)** *Dendronella articulata* Moussavian and Senowbari-Daryan; section Blejski vintgar; Carnian. **(r)** *Piallina bronnimanni* Martini et al.; section Blejski vintgar; Julian. **(s)** *Hydrania dulloi* Senowbari-Daryan; section Blejski vintgar; Carnian. **(t)** *Koskinobullina socialis* Cherchi and Schroeder; section Blejski vintgar; lower Tuvalian. **(u-v)** *Cucurbita infundibuliforme* Jablonský. (u) Section Blejski vintgar; lower Tuvalian. (v) Section Zatrnik; lower Tuvalian. **(w)** *Cucurbita longicollum* Senowbari-Daryan; section Zatrnik; lower Tuvalian. **(x)** *Cucurbita* cf. *minima* Senowbari-Daryan; section Blejski vintgar; lower Tuvalian. **(y)** *Turriglomina mesotriasica* (Koehn-Zaninetti); section Zatrnik; lower Tuvalian. (z) *Alpinophragmium perforatum* Flügel; section Poljane; lower to middle Tuvalian.

Discussion

Conodont and radiolarian data obtained in this study confirm the Longobardian age of the base of the Zatrnik Limestone. The logged succession reaches up to the Lower Norian, but basinal sedimentation clearly continued (cf. Cousin, 1981; Goričan et al., 2018). Micritic limestone with thin-shelled bivalves and radiolarians (e.g., MF 2, 3), dominating in the Zatrnik, Mt. Galetovec and Poljane sections, indicates hemipelagic sedimentation in an open marine environment. Resedimented carbonates are subordinate in these sections, but predominate in the Blejski vintgar section. Normal grading and parallel lamination suggest deposition via turbidites. Sparite-dominated varieties (MF 9, 10) are proximal turbidites, whereas micrite-rich microfacies types (MF 2, 4-7, 8, 11) are interpreted as distal turbidites (see Maurer et al., 2003). Mud-supported bioclastic-intraclastic floatstone (MF 12) and intraclastic rudstone (MF 13) might be debris-flow deposits (Mullins & Cook, 1986; Eberli, 1991). The predomination of calcarenite in the Blejski vintgar section suggests deposition in a more proximal part of the basin. Slump structures are also more common in the Blejski vintgar section. The observed transition to massive limestone in the Poljane section remains unexplained, and is also poorly dated by fossils. One possibility is that the massive bed represents a large slump, but no internal deformations were recognised and the underlying beds do not display any deformations. In view of this last argument, we rule out the possibility that the massive bed is a large block of a platform that slid into the basin. A third explanation might suggest that the section records the transition between the basin and the slope/margin of a platform. This alternative demands further explanation as to why the Zatrnik Limestone continued to deposit until the lowermost Jurassic, after which it is followed by gravity deposits. Perhaps the extent of progradation was limited, or a relative rise in sea levels led to the retreat of the platform. The answer may lie in the younger parts of the Zatrnik Limestone, which remain to be logged.

The predominance of micritic particles in resediments is common for the Middle Triassic – Early Carnian period, when carbonate platforms from slopes to tops were dominated by microbialites (Keim & Schlager, 1999; Russo, 2005; Schlager & Reijmer, 2009). Most grains (boundstone intraclasts, microproblematica) could thus have originated from the margin, slope or top of a carbonate platform (see Marangon et al., 2011). Rare fragments of green algae on the other hand surely derive from shallower parts of the adjacent platform. An increase in resedimented skeletal material is noted in late Tuvalian and/or early Norian (Mt. Galetovec and Poljane) sections. The Latest-Carnian increase in skeletal material is consistent with the conclusions of Martindale et al. (2017), who suggests that the shift towards the skeletal boundstones of the Dachstein-type reefs was gradual rather than sudden, and that the switch in dominant reef ecologies occurred during the late Carnian through early Norian interval.

The lack of siliciclastic input into the Bled Basin during the Carnian stands in contrast to the relatively closely situated Tolmin and Tarvisio Basins. Within the Tolmin Basin, clay-rich "Amphiclina beds" several tens (probably hundreds) of meters thick deposited during the Carnian. This formation is dominated by black shale alternating with lithic sandstone and hemipelagic limestone (Čar et al., 1981; Turnšek et al., 1982, 1984; Buser, 1986), whereas the uppermost part (dated as Tuvalian) consists of hemipelagic limestone alternating with black shale (Kolar-Jurk-

ovšek, 1982). In the Tarvisio Basin, the increase in the siliciclastics is reflected in the deposition of marlstone and marly limestone of the Tor Formation (Ogorelec et al., 1984; Gianolla et al., 2003; Gale et al., 2015). This is succeeded by a shallow-marine carbonate bank (the Portella Dolomite), followed by upper Tuvalian thin-bedded hemipelagic limestone and dolomite of the Carnitza Formation (Gianolla et al., 2003; Gale et al., 2015). The absence of clay input in the Bled Basin could perhaps be related to its slightly different palaeogeographic position (e.g. a position far from some river outlet), sea currents, slope steepness, etc. Alternatively, the clay-rich part of the formation could be thin and/or covered by vegetation and has thus simply not yet been recorded.

Conclusions

The Zatrnik Limestone marks the Bled Basin as a distinct paleogeographic unit. The following conclusions can be drawn from this study:

- The base of the Zatrnik Limestone is Longobardian in age.

- The Zatrnik Limestone was deposited on a basin plain and/or distal slope of the basin. The logged succession is dominated by hemipelagic limestone and distal calciturbidites. The latter are more common in the upper Julian? to lower Tuvalian. No siliciclastic-rich interval is currently recorded for the Carnian part of the formation.

- An increase in resedimented skeletal material in calciturbidites is noted in the upper Tuvalian and/or lower Norian, marking the shift from microbe-dominated to skeletal-dominated carbonate production on the platform.

Acknowledgements

This research was financially supported by the Slovenian Research Agency (Programmes No. P1-0011 and P1-0008). We thank Camille Peybernes for discussion in determination of microproblematica, Marija Petrović and Mladen Štumergar for the technical support, and students from the University of Ljubljana who attended field work and helped with logging of the sections. Reviewers are greatly acknowledged for their time, feedbacks and suggestions which led to the final state of the paper.

References

Budkovič, T. 1978: Stratigrafija Bohinjske doline. Geologija, 21: 239-244.

Buser, S. 1980: Explanatory book to Basic Geological Map SFRY 1: 100.000, Sheet Celovec (Klagenfurt). Zvezni geološki zavod, Beograd.

Buser, S. 1986: Explanatory Book to Basic Geological Map SFRY 1: 100.000, Sheets Tolmin and Videm (Udine). Zvezni geološki zavod, Beograd:103 p.

Buser, S. 1987: Basic Geological Map SFRY 1: 100.000, Sheets Tolmin and Videm (Udine). Zvezni geološki zavod.

Buser, S. 1989: Development of the Dinaric and the Julian carbonate platforms and of the intermediate Slovenian Basin (NW Yugoslavia). Mem. Soc. Geol. It., 40: 313–320.

Buser, S. 1996: Geology of Western Slovenia and its paleogeographic evolution. In: Drobne, K., Goričan, Š. & Kotnik, B. (eds.): International workshop Postojna '96: The role of impact processes and biological evolution of planet Earth. Založba ZRC, Ljubljana: 111-123.

Buser, S. 2010: Geological map of Slovenia 1:250.000. Geološki zavod Slovenije, Ljubljana.

Caggiati, M. 2014: The depositional system of Dolomia Principale/Hauptdolomit in the eastern Southern Alps: from the flattening of palaeotopography to the emplacement of the carbonate platform (Upper Triassic, NE-Italy, NW Slovenia). PhD thesis. Università degli Studi di Ferrara, Ferrara: 256 p.

Chen, Y.L., Krystyn, L., Orchard, M.J., Ali, X.L. & Richoz, S. 2015: A review of the evolution, biostratigraphy, provincialism and diversity of Middle and early Late Triassic conodonts. Papers Palaeont., 2/6: 235-263. https://doi.org/10.1002/spp2.1038

Cousin, M. 1970: Esquisse géologique des confins italo-yougoslaves: leur place dans les Dinaride set les Alpes méridionales. Bull. Soc. Géol. France, 7/12: 1034-1047.

Cousin, M. 1973: Le sillon slovène: les formations triasiques, jurassiques et néocomiennes au Nord-Est de Tolmin (Slovénie occidentale, Alpes méridionales) et leurs affinités dinariques. Bull. Soc. Géol. France, 7/15: 326-339.

Cousin, M. 1981: Les rapports Alpes-Dinarides. Les confins de l'Italie et de la Yougoslavie. Soc. Géol. Nord, 5: vol I: 1-521, vol. II Annexe: 1-521.

Čar, J., Skaberne, D., Ogorelec, B., Turnšek, D. & Placer, L. 1981: Sedimentological

characteristics of Upper Triassic (Cordevolian) circular quiet water coral bioherms in western Slovenia, northwestern Yugoslavia. SEPM Spec. Publ., 30: 233-240. https://doi.org/10.2110/pec.81.30.0233

De Zanche, V., Gianolla, P. & Roghi, G. 2000: Carnian stratigraphy in the Raibl/Cave del Predil area (Julian Alps, Italy). Eclogae Geol. Helv., 93: 331-347.

Diener, C. 1884: Beitrag zur Geologie des Zentralstockes der julischen Alpen. Jb. Kais. König. Geol. R.-A., 34: 659-706.

Doglioni, C. & Siorpaes, C. 1990: Polyphase deformation in the Col Bechei area (Dolomites –Northern Italy). Eclogae Geol. Helv., 83: 701-710.

Dozet, S. & Buser, S. 2009: Triassic. In: Pleničar, M., Ogorelec, B. & Novak, M. (eds.): The Geology of Slovenia. Geološki zavod Slovenije, Ljubljana: 161-214.

Dunham, R.J. 1962: Classification of carbonate rocks according to depositional texture. In: Han, W.E. (ed.): Classification of carbonate rocks, A symposium. American Ass. Petrol. Geol. Mem., Tulsa: 108-121.

Eberli, G.P. 1991: Calcareous turbidites and their relationship to sea-level fluctuations and tectonism. In: Einsele, G., Ricken, W. & Seilacher, D.K. (eds.): Cycles and events in stratigraphy. Springer-Verlag, Berlin Heidelberg: 45-60.

Flügel, E. 1967: Eine neue Foraminifere aus den Riff-Kalken der nordalpinen Ober-Trias: *Alpinofragmium perforatum* n. g., n. sp. Senck. Lethaea, 48: 381-402.

Gale, L. 2010: Microfacies analysis of the Upper Triassic (Norian) "Bača Dolomite": early evolution of western Slovenian Basin (eastern Southern Alps, western Slovenia). Geol. Carpathica, 61: 293-308. https://doi.org/10.2478/v10096-010-0017-0

Gale, L., Kolar-Jurkovšek, T., Šmuc, A. & Rožič, B. 2012: Integrated Rhaetian foraminiferal and conodont biostratigraphy from the Slovenian Basin, eastern Southern Alps. Swiss J. Geosci., 105/3: 435-462. https://doi.org/10.1007/s00015-012-0117-1

Gale, L., Celarc, B., Caggiati, M., Kolar-Jurkovšek, T., Jurkovšek, B. & Gianolla, P. 2015: Paleogeographic significance of Upper Triassic basinal succession of the Tamar Valley, northern Julian Alps (Slovenia). Geol. Carpathica, 66/4: 269-283. https://doi.org/10.1515/geoca-2015-0025

Geyer, G. 1900: Ueber die Verbreitung und stratigraphische Stellung der schwarzen Tropites-Kalke bei Sau Stefano in Cadore. Verh. Kaiser. König. Geol. R.-A., 15/16: 355-370.

Gianolla, P., De Zanche, V. & Mietto, P. 1998: Triassic sequence stratigraphy in the Southern Alps (Northern Italy): definition of sequences and basin evolution. In: De Graciansky, P.C., Hardenbol, J., Jacquin, T. & Vail, P.R. (eds.): Mesozoic and Cenozoc Sequence Stratigraphy of European Basins (eds.). SEPM, Spec. Publ., 60: 719-746.

Gianolla, P., De Zanche V. & Roghi, G. 2003: An Upper Tuvalian (Triassic) platform-basin system in the Julian Alps: the start-up of the Dolomia Principale (Southern Alps, Italy). Facies, 49/1: 135-150. https://doi.org/10.1007/s10347-003-0029-7

Gianolla, P., Mietto, P., Rigo, M., Roghi, G. & De Zanche, V. 2010: Carnian-Norian paleogeography in the eastern Southern Alps. Albertiana, 39: 64-65.

Goričan, Š., Košir, A., Rožič, B., Šmuc, A., Gale, L., Kukoč, D., Celarc, B., Črne, A.E., Kolar-Jurkovšek, T., Placer, L. & Skaberne, D. 2012: Mesozoic deep-water basins of the eastern Southern Alps (NW Slovenia). J. Alp. Geol., 54: 101-143.

Goričan, Š., Žibret, L., Košir, A., Kukoč, D. & Horvat, A. 2018: Stratigraphic correlation and structural position of Lower Cretaceous flysch-type deposits in the eastern Southern Alps (NW Slovenia). Int. J. Earth Sci., 107/8: 2933-2953. https://doi.org/10.1007/s00531-018-1636-4

Härtel, F. 1920: Stratigraphische und tektonische Notizen über das Wocheiner Juragebiet. Verh. Geol. Staatsanstalt, 8-9: 134-153.

Keim, L. & Schlager, W. 1999: Automicrite on steep slopes (Triassic, Dolomites, Italy). Facies, 41: 15-26.

Kolar-Jurkovšek, T. 1982: Conodonts from Amphiclina beds and Bača dolomite. Geologija, 25: 167-188.

Kolar-Jurkovšek T. & Jurkovšek B. 2019: Conodonts of Slovenia. Geološki zavod Slovenije, Ljubljana: 260 p.

Kolar-Jurkovšek, T., Buser, S. & Jurkovšek, B. 1983: Zgornjetriasne plasti zahodnega dela Pokljuke. RMZ, 30: 151-185.

Kovács, S., Sudar, M., Grădinaru, E., Gawlick, H.J., Karamata, S., Haas, J., Péro, C., Gaetani, M., Mello, J., Polák, J., Aljinović, D., Ogorelec, B., Kolar-Jurkovšek, T., Jurkovšek, B. & Buser,

S. 2011: Triassic evolution of the tectonostratigraphic units of the Circum-Pannonian Region. Jb. Geol. B.-A., 151: 199-280.

Kozur, H. 1988: Muelleritortiidae n. fam., eine charakteristische longobardische (oberladinische) Radiolarienfamilie, Teil I. Freiberger Forschungshefte, Reihe C: Geowiss., 419: 51–61.

Kozur, H. & Mostler, H. 1994: Anisian to Middle Carnian radiolarian zonation and description of some stratigraphically important radiolarians. Geol. Paläont. Mitt. Innsbruck, Sdb. 3: 39-255.

Kozur, H.W. & Mostler, H. 1996: Longobardian (Late Ladinian) Oertlispongidae (Radiolaria) from the Republic of Bosnia-Herzegovina and the stratigraphic value of advanced Oertlispongidae. Geol. Paläont. Mitt. Innsbruck, Sdb. 4: 105-193.

Kristan-Tollmann, E. 1990: Rhät-Foraminiferen aus dem Kuta-Kalk des Gurumugl-Riffes in Zentral-Papua/Neuguinea. Mitt. Österr. Geol. Ges., 82: 211-289.

Krystyn, L., Lein, R., Schlaf, J. & Bauer, F.K. 1994: Über ein neues obertriadisch--jurassisches Intraplatformbecken in den Südkarawanken. In: Lobitzer, H., Császár, G. & Daurer, A. (eds.): Jubiläumsschrift 20 Jahre Geologische Zusammenarbeit Österreich-Ungarn. Geologische Bundesanstalt, Wien: 409-416.

Kukoč, D., Goričan, Š. & Košir, A. 2012: Lower Cretaceous carbonate gravity-flow deposits from the Bohinj area (NW Slovenia): evidence of a lost carbonate platform in the Internal Dinarides. Bull. Soc. Géol. France, 183: 383–392. https://doi.org/10.2113/gssgfbull.183.4.383

Lein, R., Schlaf, J., Müller, P.J., Krystyn, L. & Jesinger, D. 1995: Neue Daten zur Geologie des Karawanken-Strassentunnels. Geol.-Paläont. Mitt. Innsbruck, 20: 371-387.

Lieberman, H.M. 1978: Carnitza Formation. Mitt. Ges. Geol. Bergbaustud. Österr., 25: 35-60.

Marangon, A., Gattolin, G., Della Porta, G. & Preto, N. 2011: The Latemar: A flat-topped, steep fronted platform dominated by microbialites and synsedimentary cements. Sed. Geol., 240: 97-114. https://doi.org/10.1016/j.sedgeo.2011.09.001

Martindale, R.C., Foster, W. & Velledits, F. 2017: The survival, recovery, and diversification of metazoan reef ecosystems following the end--Permian mass extinction event. Palaeogeogr., Palaeoclimatol., Palaeoecol., 513: 100-115. https://doi.org/10.1016/j.palaeo.2017.08.014

Matzner, C. 1986: Die Zlambach-Schichten (Rhät) in den Nördlichen Kalkalpen: Eine Platform-Hang-Beckenentwicklung mit allochthoner Karbonatsedimentation. Facies, 14: 1-104.

Maurer, F., Reijmer, J.J.G. & Schlager, W. 2003: Quantification of input and compositional variations of calciturbidites in a Middle Triassic basinal succession (Seceda, Dolomites, Southern Alps). Int. J. Earth Sci., 92/4: 593-609. https://doi.org/10.1007/s00531-002-0301-z

Mullins, H.T. & Cook, H.E. 1986: Carbonate apron models: Alternatives to the submarine fan model for paleoenvironmental analysis and hydrocarbon exploration. Sed. Geol., 48: 37-79.

Ogorelec, B., Jurkovšek, B., Šribar, L., Jelen, B., Stojanovič, B. & Mišič, M. 1984: Carnian beds at Tamar and at Log pod Mangartom. Geologija, 27: 107-158.

Placer, L. 1999: Contribution to the macrotectonic subdivision of the border region between Southern Alps and External Dinarides. Geologija, 41: 223-255. https://doi.org/10.5474/geologija.1998.013

Placer, L. & Čar, J. 1998: Structure of Mt. Blegoš between the Inner and Outer Dinarides. Geologija, 40: 305-323.

Poli, M.E. & Zanferrari, A. 1995: Dinaric thrust tectonics in the Southern Julian Prealps (Eastern Southern Alps, NE Italy). In: Vlahović, I. (ed.): Proceedings of the first Croatian Geological Congress, Opatija 18-21-10.1995, 2. Institute of Geology & Croatian Geological Society, Zagreb: 465-468.

Ramovš, A. 1986: Paläontologisch bewiesene Karn/Nor-Grenze in den Julischen Alpen. Newslett. Strat., 16: 133-138.

Ramovš, A. 1998: Conodonten-Stratigraphie der Obertrias von Slowenien: Ergebnisse eidener Untersuchungen. Geologija, 40: 223-232. https://doi.org/10.5474/geologija.1997.009

Rigo, M., Mazza, M., Karádi, V. & Nicora, A. 2018: New Upper Triassic conodont biozonation of the Tethyan realm. In: Tanner, L.H. (ed.): Topics in Geobiology, 46: 189-235. https://doi.org/10.1007/978-3-319-68009-5_6

Rožič, B. 2009: Perbla and Tolmin formations: revised Toarcian to Tithonian stratigraphy of the Tolmin Basin (NW Slovenia) and regional correlations. Bull. Soc. Géol. France, 180: 411-430.

Rožič, B., Kolar-Jurkovšek, T. & Šmuc, A. 2009: Late Triassic sedimentary evolution of

Slovenian Basin (eastern Southern Alps): description and correlation of the Slatnik Formation. Facies, 55: 137-155.

Rožič, B., Kolar-Jurkovšek, T., Žvab Rožič, P. & Gale, L. 2017: Sedimentary record of subsidence pulse at the Triassic/Jurassic boundary interval in the Slovenian Basin (eastern Southern Alps). Geol. Carpathica, 68: 543-561. https://doi.org/10.1515/geoca-2017-0036

Russo, F. 2005: Biofacies evolution of the Triassic platforms of the Dolomites, Italy. Ann. Univ. Studi Ferrara Mus. Sci. Natur., Vol. Spec. 2005: 33-44.

Schlaf, J. 1996. Ein obertriadisches Intraplattformbecken aus den Südkarawanken (Kärnten, Östereich). Mitt. Ges. Geol. Bergbaustud. Österr., 39/40: 1-14.

Schlager, W. & Reijmer, J.J.G. 2009: Carbonate platform slopes of the Alpine Triassic and the Neogene - a comparison. Austrian J. Earth Sci., 102: 4-14.

Turnšek, D., Buser, S. & Ogorelec, B. 1982: Carnian coral-sponge reefs in the Amphiclina beds between Hudajužna and Zakriž (western Slovenia). Razprave IV razreda SAZU, 24: 51-98.

Turnšek, D., Buser, S. & Ogorelec, B. 1984: The role of corals in Ladinian-Carnian reef communities of Slovenia, Yugoslavia. Paleont. Americana, 54: 201-209.